PSERC

Analysis and Design of Power Acceptability Curves for Industrial Loads

Masters Thesis and
Final Project Report

Power Systems Engineering Research Center

A National Science Foundation
Industry/University Cooperative Research Center
since 1996

Cornell • Arizona State • Berkeley • Carnegie Mellon • Colorado School of Mines
Georgia Tech • Illinois • Iowa State • Texas A&M • Washington State • Wisconsin

Analysis and Design of Power Acceptability Curves for Industrial Loads

Thesis and Final Report

John Kyei

PSERC Publication 01-28

February 2001

Information about this Thesis and Project Report

This thesis was prepared under the direction of:

Gerald T. Heydt
Professor
School of Electrical Engineering
Arizona State University
Tempe, AZ 85287-5706
Phone: 480-965-8307
Fax: 480-965-0745
e-mail: heydt@asu.edu

The thesis serves as the final report for the PSERC project "Redesign and New Interpretation of Power Acceptability Curves for Three Phase Loads."

Additional Copies of the Report

Copies of this thesis can be obtained from the Power Systems Engineering Research Center's website, www.pserc.wisc.edu. The PSERC publication number is 01-28. For additional information, contact:

Power Systems Engineering Research Center
Cornell University
428 Phillips Hall
Ithaca, New York 14853
Phone: 607-255-5601
Fax: 607-255-8871

Notice Concerning Reproduction

ACKNOWLEDGEMENTS

My heartfelt gratitude first goes to Dr. G. T. Heydt, Professor Arizona State University, who supervised this project. I am highly impressed with his guidance and simplicity of suggestions, which really contributed to the success of this research work.

Next, I acknowledge Dr. Raja Ayyanar, Associate Professor Arizona State University for his valuable and immense contribution to the success of this work.

Many engineers contributed to the success of this work. I would especially like to thank Dr. Rao Thallam, John Blevins, Barry Cummings, Kristiaan Koellner, Thomas LaRose, and Steven Sturgill, all of Salt River Project for their critical review and suggestions. My special thanks go to Dr. Peter Sauer of the University of Illinois and Dr. A.P.S. Meliopoulos of Georgia Technical Institute for reviewing this work.

Finally, I would like to thank Salt River Project for their financial support and provision of field data.

The work described in this thesis was sponsored by the Power Systems Engineering Research Center (PSERC). We express our appreciation for the support provided by PSERC's industrial members and by the National Science Foundation through the grant NSF EEC-0001880 to Arizona State University received under the NSF Industry/University Cooperative Research Center program.

EXECUTIVE SUMMARY

There has been a concern in recent years for electric power utilities to satisfy the increasingly expectations of not only the industrial and commercial, but also the residential users with respect to the quality of the supplied energy. This concern calls for the redesigning of the existing power quality indices to capture all the industrial, commercial and household loads, which hitherto has not been considered. Several electric power indices have evolved over the years as tools to represent, quantify and measure a complex issue at hand. The use of these indices is widespread in the field of electric power generation, transmission and distribution.

Another way of quantifying power quality issues is the use of power acceptability curves. These curves are plots of bus voltage deviation versus time duration. And they separate the bus voltage deviation - time duration plane into two regions: an “acceptable” and “unacceptable”. Various power acceptability curves exist but the most widely publicized one, which could stand the test of time and could be relied on, is the Computer Business Equipment Manufacturers Association or CBEMA curve. The CBEMA curve has been in existence since 1970’s. Its primarily intent was to give a measure of the vulnerability of mainframe computer to the disturbance in the electric power supply. But the curve has been used as a measure of power quality indices for electric drives and solid-state loads.

In this report, the concept of 'standards' is introduced for the design of power acceptability curves. The power acceptability curves are aides in the determination of whether the supply voltage to a load is acceptable for the maintenance of a load process. The construction of the well known CBEMA power acceptability curve is discussed, and issues of three phase and rotating loads are discussed.

The main conclusion of this work is that power acceptability curves can be designed to detect compliance or noncompliance of the distribution supply to effect a standard. If the load is a rectifier load, the standard is generally the permissible low threshold of DC voltage at the rectifier output. Other standards are possible including a speed standard for rotating loads. The general process of the design of a power acceptability curve entails the solution of a dynamic model for the load. The dynamic solution then gives a standard parameter versus time, and this is compared with the ultimate standard (e.g., V_{dc} = 0.87 per unit). This gives a permissible duration of a voltage sag event. The method is easily extended to the unbalanced three phase case.

It is shown in the report that the CBEMA curve is effectively based on a single phase rectifier load with DC threshold voltage of 0.87 per unit in the undervoltage region. A double exponential equation describing the curve is developed. This provides a useful method to consider the effect of unbalanced voltage sags and to develop CBEMA-like curves for other types of loads.

A scalar index of compliance with a power acceptability curve has been illustrated in this report as well.

TABLE OF CONTENTS

CHAPTER Page

LIST OF TABLES

LIST OF FIGURES

NOMENCLATURE

abc	Conventional *a*-*b*-*c* axes
AC	Alternating current
ANSI	American National Standards Institute
ASD	Adjustable speed drive
b	Time constant
$B\omega$	Viscous friction
C	Capacitance
c	Time constant
CBEMA	Computer Business Equipment Manufacturers Association
DC	Direct current
dqO	Direct and quadrature axes
ES	Energy served
F	Filter
FIPS	Federal Information Processing Standards
I_1	Steady state stator current
I_2	Steady state rotor current
i	Instantaneous current
I_{pa}	Proposed index of power acceptability
IEEE	Institute of Electrical and Electronic Engineers
ITIC	Information Technology Industry Council
J	Moment of inertia
j	$\sqrt{-1}$
K	Load torque constant

L	Inductance
MATLAB®	MATrix LABoratory: Software package for high-performance numerical computations
NEMA	National Electrical Manufacturers Association
P	An operating point
PF	Power factor
PSpice®	Simulation package for circuit analysis
pu	Per unit
R	Resistance
r_1	Stator resistance
r_2	Rotor resistance
R_{dc}	DC resistance
r_m	Core and magnetizing branch resistance
RMS	Root mean square value of a function
s	Induction machine slip in per unit
SARFI	System Average RMS Frequency Index
SCR	Silicon controlled rectifier
SEI	Sag energy index
SEMI	Semiconductor Equipment Materials International
T	Disturbance duration in seconds
T_e	Shaft torque in Newton-meter
T_L	Load torque in Newton-meter
THD	Total harmonic distortion
v	Instantaneous voltage

V	Bus voltage
V_+	Positive sequence component of bus voltage
V-	Negative sequence component of bus voltage
V_{ac}	AC voltage
V_{dc}	DC voltage
V_{end}	Ultimate voltage ($t \rightarrow \infty$)
V_T	Threshold voltage
VUF	Voltage unbalance factor
W	Disturbance energy
x_1	Stator reactance
x_2	rotor reactance
x_m	Core and magnetizing branch reactance
ΔV	Voltage sag
ω	Shaft speed of induction machine in radians per second
ω_s	synchronous speed of the induction machine in radians per second

Chapter 1

Introduction

1.1 Motivation

There has been a concern in recent years for electric power utilities to satisfy the increasing expectations of not only industrial and commercial, but also residential users with respect to the quality of supplied electrical energy. Power quality relates to the ability of the user to utilize the supplied energy from the secondary power distribution system or, in some cases, from the primary distribution or even the transmission system. There are a number of approaches to the quantification of power quality including:

- The cost to "condition" the power supplied
- The costs associated with the failure of industrial processes when these failures are due to power quality
- The formulation of power quality indices and other metrics that measure various aspects of the supplied voltage.

In this thesis, attention is focused on one type of power quality measure, the power acceptability curve. The focus calls for the analysis, design, and redesign of power acceptability curves to capture critical aspects of the power supply. These critical elements depend on the sector of the load served (industrial, commercial, residential), and the specific loads served. Some critical measures of power quality may be totally innovative. The concept of an index based on compliance with a power acceptability curve is proposed.

1.2 Research objectives

The main objectives of this research are the analysis, extension, understanding and modification of the power acceptability curves (e.g., the Computer Business Equipment and Manufacturers Association or CBEMA curve and Information Technology Industry Council or the ITIC curve) to permit accurate application in the case of three phase loads. A section of this chapter is dedicated to the detailed description of these curves. It is an objective to fully analyze these curves from the point of view of energy disturbance. Alternative power acceptability curves are suggested for different loads. Three phase applications are considered in terms of certain transformed variables (e.g., symmetrical components, and Clarke components). An objective result of the work is a method applicable to short and longer transient voltage sags for classification as 'acceptable' or 'unacceptable' in terms of the power acceptability curves.

An additional objective of this research is the development of an index that captures the degree of compliance of distribution power with the power acceptability curves.

1.3 Scope of research

The project scope includes the following:

- Analysis of the CBEMA and ITIC curves in the three-phase case.
- Studies of three phase unbalanced magnitude and unbalanced phase angles.
- Negative and zero sequence effects.
- Effects of sags on the energy transferred to electronically switched loads.
- Development and assessment of indices that measure the compliance of distribution of power with power acceptability curves.

- The voltage level application is mainly 480V secondary distribution voltages for industrial loads.

1.4 Power quality indices and the power acceptability curves

Several electric power indices have evolved over the years as tools to represent, quantify and measure a complex issue at hand. The use of these indices is widespread in the field of electric power generation, transmission and distribution. Some of the electric power quality indices and their applications are depicted in Table 1.1.

Another way of quantifying power quality issues is the use of power acceptability curves. These curves are plots of bus voltage deviation versus time duration. And they separate the bus voltage deviation - time duration plane into two regions: an “acceptable” and “unacceptable”. Various power acceptability curves exist but the most widely publicized is the CBEMA curve. The CBEMA curve has been in existence since the 1970s [1]. Its primary intent was to give a measure of the vulnerability of mainframe computer to the disturbance in the electric power supply. But the curve has been used as a measure of power quality for electric drives and solid-state loads as well as a host of wide-ranging residential, commercial, and industrial loads. The CBEMA curve was redesigned in 1996 and renamed for its supporting organization, the Information Technology Industry Council [1]. The CBEMA, Figure 1.1 and the newer ITIC curve, Figure 1.2 have everything in common with the exception of the way the acceptable operating region is represented. Whereas CBEMA represents the acceptable region by a curve, ITIC depicts the region in steps. Table 1.2 lists several alternative power acceptability curves [1].

Table 1.1 Common power quality indices [3-4,10]

Index	Definition	Main applications
Total harmonic distortion (THD)	$\left(\sqrt{\sum_{i=2}^{\infty} I^{2}{}_{i}} \right) / I_{1}$	General purpose; standards
Power factor (PF)	$P_{tot} / \left(\lvert V_{RMS} \rvert \lvert I_{RMS} \rvert \right)$	Revenue metering
Telephone influence factor	$\left(\sqrt{\sum_{i=2}^{\infty} w_{i}^{2} I_{i}^{2}} \right) / I_{1}$	Audio circuit interference
C message index	$\left(\sqrt{\sum_{i=2}^{\infty} c_{i}^{2} I_{i}^{2}} \right) / I_{RMS}$	Communications interference
IT product	$\sqrt{\sum_{i=1}^{\infty} w_{i}^{2} I_{i}^{2}}$	Audio circuit interference; Shunt capacitor stress
VT product	$\sqrt{\sum_{i=1}^{\infty} w_{i}^{2} V_{i}^{2}}$	Voltage distortion index
K factor	$\left(\sum_{h=1}^{\infty} h^{2} I_{h}^{2} \right) / \left(\sum_{h=1}^{\infty} I_{h}^{2} \right)$	Transformer derating
Crest factor	V_{peak} / V_{RMS}	Dielectric stress
Unbalance factor	$\lvert V_{-} \rvert / \lvert V_{+} \rvert$	Three phase circuit balance
Flicker factor	$\Delta V / \lvert V \rvert$	Incandescent lamp operation; Bus voltage regulation

Table 1.2 Alternative power acceptability curves [1]

Curve	Year	Application
ITIC curve	1996	Information technology equipment
IEEE Emerald Book	1992	Sensitive electronic equipment
CBEMA curve	1978	Computer business equipment
FIPS power acceptability curve	1978	Automatic data processing equipment
AC line voltage tolerances	1974	Mainframe computers
Failure rates curve for industrial loads	1972	Industrial loads

1.5 The CBEMA and ITIC curves

The CBEMA power acceptability curve is a graphical representation of bus voltage amplitude deviation from rated value, applied to a power circuit versus the time factor involved [2]. Figure 1.1 depicts a CBEMA curve, where the ordinate is shown in percent, that is a percent deviation from rated voltage. Thus the rated bus voltage is represented by the $\Delta|V| = 0$ axis. The abscissa depicts the time duration for the disruption, which is usually expressed in either cycles or seconds. In this case, it is expressed in seconds. It could be seen that the curve has two loci: the overvoltage locus above the $\Delta|V| = 0$ axis and the undervoltage locus below the axis. In the center is an acceptable power area. Steady state is at $t \to \infty$ and short-term events occur to the left on the time axis. Overvoltages and undervoltages of shorter durations are tolerable if the events are within the acceptable region. The guiding principle is that if the supply voltage stays within the acceptable power area then the sensitive equipment will operate

well. However, if such an event persist for a longer time then the sensitive equipment might fail.

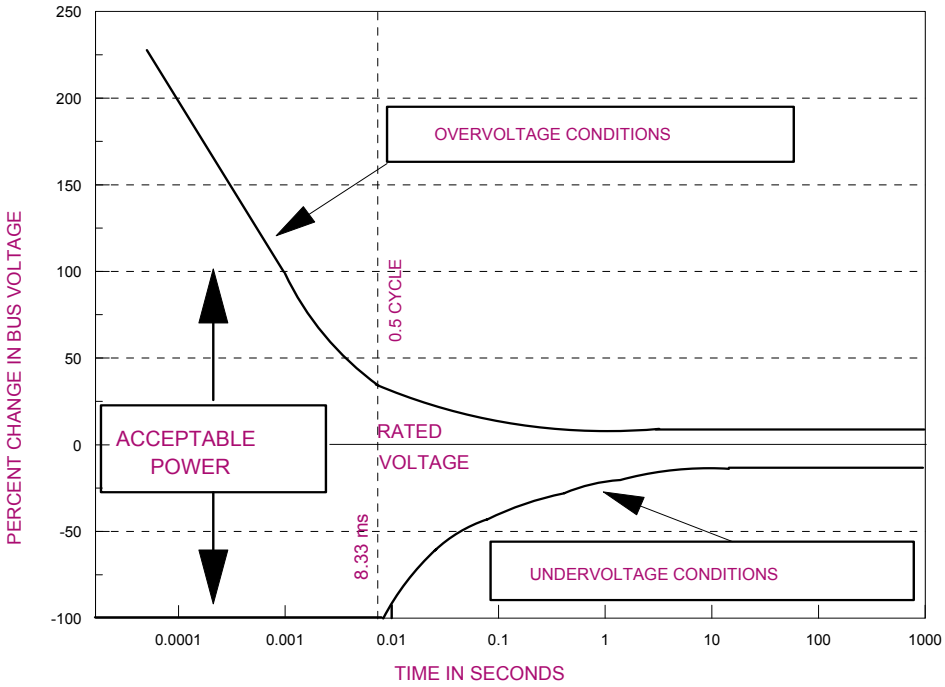

Figure 1.1 The CBEMA power acceptability curve

The ITIC power acceptability curve depicted in Figure 1.2 is a revision of the earlier CBEMA curve. The CBEMA curve seems to nonetheless enjoy widespread use as an equipment benchmark for power supplies since the late 1970s and the CBEMA curve was adopted as a voltage sag ride-through benchmark for comparison to equipment immunity. The ITIC curve has an expanded acceptable power area or operating region for the portions of $\Delta|V| - t$ plane. And instrumentation to check compliance with the ITIC curve appear to be easier to design because of the simplified way the acceptable region is represented. Like the CBEMA curve, the ITIC curve is recommended as a design tool for manufacturers of computer equipment [1].

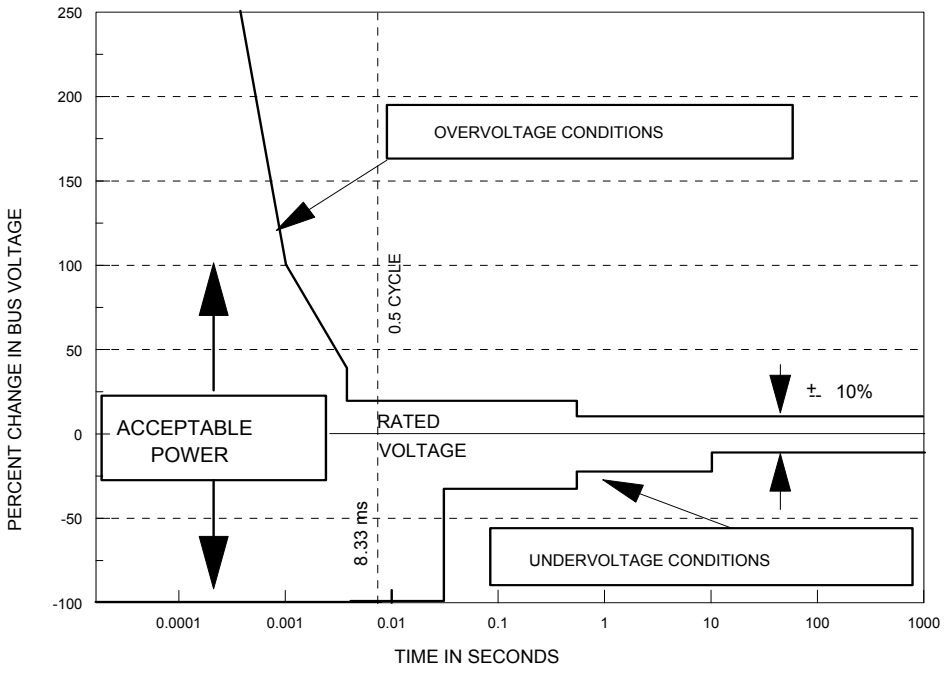

Figure 1.2 The ITIC power acceptability curve

The applicability of these curves to single phase loads has been addressed in most literature. The issue now is how these curves could be modified and redesigned to accommodate three phase effects, since virtually all transmission and most primary distribution systems are three-phased in nature. For this reason most of the industrial and commercial loads are energized by three phase supply. This brings into focus the development of a method that will classify short and longer transient voltage sags as ‘acceptable’ or ‘unacceptable’ in terms of power acceptability curves.

Over the past decade, most of the installed industrial and commercial equipment such as adjustable speed drives (ASDs), programmable logic controllers, starters, digital clocks have been electronic in nature and are sensitive to voltage sags events. There is a need to develop a parameter or set of parameters that will capture the severity of a

voltage sag event in order to protect installed equipment. The parameter must be able to account for both balanced and unbalanced faults.

1.6 Literature review

Electric utility companies receive complaints about the sensitivity of some industrial equipment to voltage fluctuation [7]. There is the need for reexamination of the indicators that measure the quality of supplied voltage. Several electric power quality indicators and standards have been discussed in the literature [1,7]. Stephen and McComb [7] published that the lower portion of the ITIC curve and the new SEMI F47 (specification for semiconductor processing equipment voltage sag immunity) standard are the two most important standards to consult in dealing with power quality issues in chiller systems. It was also stressed that the design of control components such as power supplies, relays, contactors, motor starters and adjustable speed drives, which are common in industry, in particular chiller systems must adhere to the two stringent standards.

However, the pitfalls of these electric power quality indices need to be studied before their application [3]. Waggoner [2] established in his publication that a detail understanding of CBEMA curve is vital in combating power quality problems, with assurance of optimum operation of sensitive electronic equipment. The application of power acceptability curves, specifically CBEMA curve to single phase loads has been detailed in most of the technical documents. Their application to three phase loads is however, being looked into. Thallam and Heydt [1] discussed the use of power acceptability curves for assessing and measuring bus voltage sags with reference to three phase loads. The applicability of the power acceptability curves to selected three phase

loads was outlined. In particular, it was recommended that positive sequence supply voltage be used in employing power acceptability curves to assess the quality of power supply to three phase loads that are AC to DC converters. This is due to the fact that the negative and zero sequence supply do not result in energy fed to the load. The problem here is the method to calculate the positive sequence component of voltage from three phase time domain data. Application of power acceptability curves to other three phase load types such as induction motor loads driven directly from AC bus, line commutated three phase rectifier loads, forced commutated three phase rectifier loads and pulse width modulated drives for induction motors have been explored in [6]. It became clear in this case that positive and negative sequence voltages at the load bus needed to be considered when treating voltage sags caused by unbalanced three phase faults. Ride through issues for DC motor drives during voltage sags are discussed in [12].

A model based on constant energy concept was derived for power acceptability curves [6]. This model assumed that disturbances to loads, whether they are as a result of overvoltage or undervoltage events will have an impact depending on how much excess energy is delivered to the load (in the overvoltage case) or how much was not delivered to the load (in the undervoltage case). From this model, the locus of the power acceptability curve was obtained to be of the form,

$$W = |V|^k T$$

where W is the threshold energy to cause a load disruption, T is the duration of the disturbance, and V is the bus voltage during the disturbance. The problem with this constant energy concept is that the energy delivery by the bus voltage is purely load dependent. For a quick example, $k = 1$, for constant current loads, for constant impedance

or resistive loads, $k = 2$. Load characteristics also play a great role on the level of the threshold energy. That is sensitive loads have smaller values of W, while insensitive loads will have higher values of W. It arises from the constant energy concept that the relation below approximates the undervoltage limb of the CBEMA curve,

$$\left(\Delta|V|\right)^{3.142} T = 12455$$

where $\Delta|V|$ is in percent and T is in seconds. These numerical values are found assuming the $\Delta|V|^k T$ form and using a logarithmic graph as shown in Figure 1.3 to find k and W. Since a simple linear form is used in Figure 1.3, a mean square fit is used to identify k and $log\ W$.

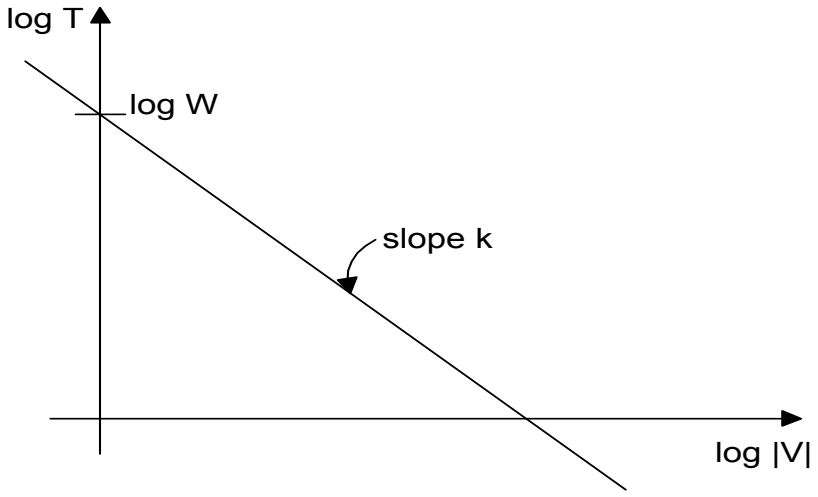

Figure 1.3 Logarithmic representation of the relation $W = \Delta|V|^k T$

The CBEMA curve stipulates that equipment should be able to ride through zero volts for half a cycle. This suggests that a sub cycle response to voltage sags is a requirement for the prevention of the malfunctioning of certain types of equipment. Static switches such SCRs (silicon controlled rectifiers) do offer such a response for majority of the circumstances but cannot react quickly to all the sag events to which they

are subjected. Their response is limited by the need to process the voltage and current information to determine the state of the system [11]. In addition, two types of delays could be identified, one relates to the finite time to reverse bias the switches and the other has to do with the detection method employed. A popular detection method is the *dqO* transform. The *dqO* transformation is a phasor transformation that is complex and requires steady state analysis. The *dqO* transform is derived from Park's transformation for rotating machines. An alternative is to use a purely real transform, which avoids the requirement of steady state operation. Clarke's transform is such a transformation [11]. Clarke's transform of the three phase *abc* system is of the form,

$$\begin{bmatrix} V_\alpha \\ V_\beta \\ V_0 \end{bmatrix} = \frac{2}{3}\begin{bmatrix} 1 & -\frac{1}{2} & -\frac{1}{2} \\ 0 & -\frac{\sqrt{3}}{2} & \frac{\sqrt{3}}{2} \\ \frac{1}{2} & \frac{1}{2} & \frac{1}{2} \end{bmatrix}\begin{bmatrix} V_a \\ V_b \\ V_c \end{bmatrix}.$$

The voltages V_α and V_β are orthogonal vectors. The single quantity V_{dqO} could be used to represent the *abc* system as

$$V_{dqO} = \sqrt{V_\alpha{}^2 + V_\beta{}^2}\ .$$

Ennis and O'Leary established in [11] that even with the *dqO* transform detection method the quarter cycle transfer for SCR is not achievable under all circumstances. This is as a result of the fact that the transfer time of the switch is dependent on both the distribution system and the control system variables such as sag point-on-wave, sag depth and the power factor. It is recommended that a rigorous test schedule that examines these variables should be part of equipment specification. With the assertion that *dqO* transform detection method unachievable under all circumstances the depiction of the severity of voltage sag event, an objective of this work is very crucial to utilities.

To depict the severity of a voltage sag event, a voltage sag index has to be developed. Several methods has been proposed and developed as a means of qualifying sag events for the purpose of developing a composite index. In one method [9], developed by Detroit Edison, qualifying sag has at least one phase of the three-phase system equal to or below 0.75 per unit. This means that sags with minimum voltage above 0.75 per unit are not counted. In another method developed by Thallam and Heydt [1], for sag event to qualify for sag index calculation it must lie between 85% and 10%.

Several methods have been developed and employed in calculating voltage sag index. The most prominent among them are reviewed below.

- The Detroit Edison sag score method [1,9] is perhaps the first method to be used by a utility company to index low voltage conditions. The sag score is defined in terms of the root mean square (RMS) values of the phase voltages Va, Vb and Vc as

$$Sag\ Score = 1 - \frac{|Va| + |Vb| + |Vc|}{3}.$$

The strength of this method lies in the simplicity of its computation. However the method does not take into consideration the duration of the sag event, which will indicate its impact on loads. It must be noted that in this method, the voltage sag data is aggregated for a 15-minute duration at each location. And if one or two phases are greater than 1.0 per unit, they are reset to 1.0 per unit. This is the result of neutral shift. The Detroit Edison sag score does not capture phase information. Also, apart from a heuristic notion of deviation of phase-neutral voltage, there is no "scientific" or engineering basis of this score.

- System Average RMS (Variation) Frequency Index ($SARFI_x$) [5,8] is one of several indices which are already being used by utilities to address service quality issues. $SARFI_x$ represents the average number of specified RMS variation measurements events that occurred over the assessment period per customer served, where the specified disturbances are those with magnitude less than x for dips and more than x for swells,

$$SARFI_x = \frac{\sum N_i}{N_t},$$

where, x is the RMS voltage threshold, N_i, the number of customers experiencing short duration voltage deviations with magnitudes above x% for $x>100$ or below x% for $x<100$ due to measurement event i. The parameter N_i represents the number of customers served from the section of the assessed system. The advantage of the $SARFI_x$ index is that it allows for the assessment of RMS variations of a specified voltage level. Thus, it is always defined with respect to the voltage threshold x. For an example, if a utility has customers whose disturbance susceptibility to voltage sags is below 70% of the nominal supply voltage, then this disturbance group can be assessed using $SARFI_{70}$. The shortfall of this index is that it is applicable for short-duration variations in RMS voltage. Another problem is that the method does not capture three phase events. Other indices which are subsets of $SARFI_x$ and which assess variations of specified magnitude and IEEE 1159 duration category are detailed in [5]. A disadvantage of *SARFI* is that apart from a statistical account of bus voltage sags, *SARFI* does not truly measure energy, power, or any quantitative load disruption.

- Thallam and Heydt proposed an index, based on the energy lost during a voltage sag event [1]. This method called Voltage Sag-Lost Energy index (VLSEI) takes into consideration the voltage dips in all the three phases and their duration. The lost energy in a sag event or the energy that was not delivered by the system to the load during a sag event, W is calculated as

$$W = \left(1 - V_{pu}\right)^{3.14} T$$

where V_{pu} is the phase voltage magnitude in per unit of the nominal voltage during a sag event, and T is the sag duration in seconds. The power of the voltage, 3.14 was approximated from the CBEMA curve.

This work develops a voltage sag index that takes in to consideration both magnitude and duration of a sag event. This index addresses three phase issues and accounts for both balanced and unbalanced faults.

1.7 Applicable standards

There are many possible causes of voltage sag or swell events in electrical system including line switching surges, lighting impulses, line to ground faults, unbalanced single phase loads, high impedance connections and malfunctioning of voltage regulators. The immunity of sensitive electrical systems to these events is addressed in ITIC/CBEMA 1996 curve and SEMI F47 standard. Voltage unbalance events are contained in NEMA MG-1-1988 and ANSI standard C84.1-1989 [7]. Other applicable standards useful to this work are:

1) IEEE 1100, IEEE recommended practice for powering and grounding sensitive electronic equipment.
2) IEEE 1250, IEEE Guide for service to equipment sensitivity to momentary voltage disturbances.
3) IEEE 1346, Electric power compatibility with electronic process equipment.

Chapter 2

Energy disturbance concept

2.1 Introduction

Different types of electrical equipment behave in different ways under voltage sag events. The impact of a voltage sag disturbance depends on the sensitivity of the equipment to voltage sags. Energy disturbance concept is a concept based on the fact that disturbances to load depend on how much energy is delivered to the load [6]. Two types of events arise from voltage sag disturbances: an overvoltage and undervoltage event. An overvoltage event will result if excess energy is delivered to the load during the disturbance. On the other hand, a shortfall in energy delivered will account for an undervoltage event. If the cited excess or shortfall in energy is too great, the operation of the load may be disrupted. The power acceptability curves may be thought of as loci of constant energy. The energy disturbance concept may be used to model the shape of the power acceptability curves.

The objective of this chapter is to fully analyze the CBEMA curve based on the energy disturbance concept. The approach involves studying a line commutated three phase rectifier load under different loads and conditions. PSpice software is used for simulation and verification of concepts.

2.2 Line commutated three phase rectifier loads

Figure 2.1 depicts a line commutated rectifier. For the purposes of illustrating the energy disturbance concept, this load is used as an example. Specific values of the voltage supply and load are used to illustrate the main points. The rectifier receives its supply from a three phase, 480 V *AC* supply system. For the purpose of analysis, the rectifier can be considered to composed of two halves: an upper half and a lower half. The upper half comprises of the diodes D_1, D_3 and D_5. Diodes D_2, D_4 and D_6 make up the lower half. The operation of the rectifier depicted in Figure 2.1 is as follows: One of the diodes D_1, D_3 and D_5 (with high positive voltage at its anode) conducts with the application of the supply voltage. Similarly, one of the diodes D_2, D_4 and D_6 (with high negative voltage at its anode) conducts and returns the load current. The sequence of conduction of the diodes in the upper half of the bridge is D_1, D_3, D_5. Likewise, in the lower half of the bridge, the sequence is D_2, D_4, D_6. If the load current is assumed to be continuous at all times, then each diode will conduct for 120° in each half cycle of the *AC* waveform, followed by 240° of non conduction. Considering the two halves together, each diode enters conduction 60° after its predecessor in the sequence D_1, D_2, D_3, D_4, D_5, D_6. Hence the choice of the numbering scheme of the diodes in Figure 2.1.

When any of the diodes connected with the upper (positive) rail conducts, the potential of the rail is the corresponding *AC* line voltage less the forward voltage drops of the conducting diodes. Also, when any of the diodes connected with the lower (negative) rail conducts, the potential of the rail will be the corresponding *AC* line voltage minus the forward voltage drops of the conducting diodes. The voltage across the load is the difference between the positive and the negative rail potentials.

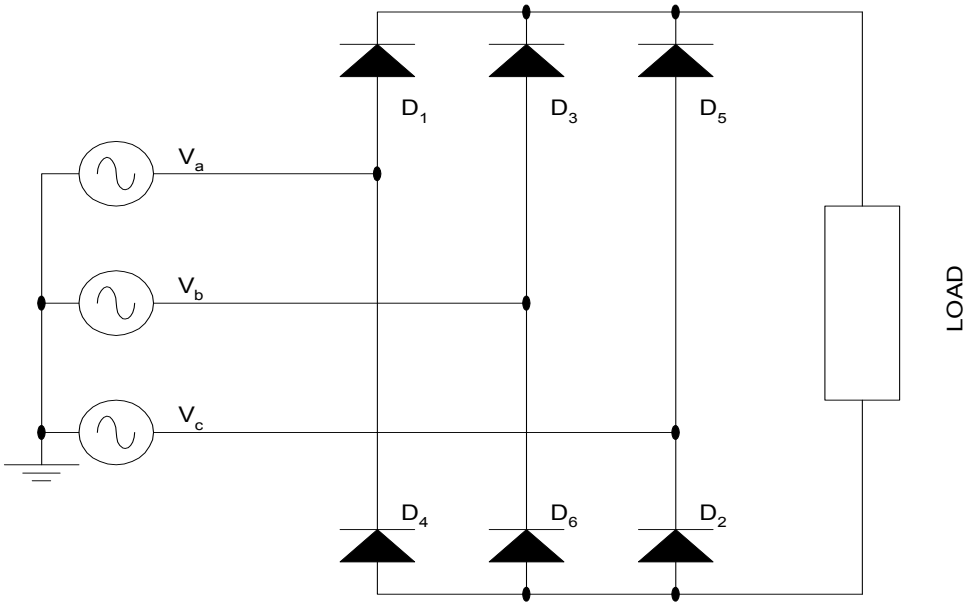

Figure 2.1 Schematic diagram of six-pulse diode bridge rectifier

When a voltage sag event occurs, the supply voltage may alter in magnitude and or in phase depending on nature of the fault. The energy that was not delivered to the load as a result of the voltage sag is called the disturbance energy, and it depends on the nature of the load, the type of voltage sag and the duration of the sag event.

2.3 Causes of voltage sags

Voltage sag is a reduction in the root mean square (RMS) of the system voltage. Voltage sags are characterized by magnitude and duration. Voltage sag events are caused by mainly short-circuit faults somewhere in the transmission and distribution system. Starting of large motors can also result in undervoltages, but these are typically longer in duration and the associated voltage magnitudes are often not very low. Voltage sags can be classified as balanced or unbalanced depending on the nature of the phase-neutral voltages. If the voltages on the three phases sag equally, then balanced sag results.

However, if the phase voltages have unequal voltage magnitudes or phase relationships other than 120°, the sag is considered as unbalanced.

Three phase short circuits and large motors such as induction motors starting may cause balanced three phase sags. Unbalanced sags are as a result of lightning, animals, trees and auto accidents, just to mention a few. Three types of unbalanced voltage sags could be identified. These are voltage sags resulting from single phase-to-ground faults, phase-to-phase faults, and phase-to-phase-to-ground faults.

In this chapter the analysis is however restricted to the effect of balanced three phase faults and unbalanced single phase-to-ground faults on the energy delivered to a six-pulse bridge rectifier with a pure resistive, inductive and capacitive loads.

2.4 Voltage sag and disturbance energy

During voltage sag, the voltage is below normal for some period of time, which leads a reduction in the power and the energy delivered to the load. The disturbance energy is the difference in energy between the actual energy delivered to the load during the sag duration and the energy that would have been delivered if the load had been supplied with the normal system voltage over the period. Mathematically, in the case of a simple resistive load in a DC circuit, the disturbance energy, W may be defined as

$$W = \frac{V_{dc,rated}^2}{R} T - \frac{V_{dc,faulted}^2}{R} T$$

where, $V_{dc,rated}$ and $V_{dc,faulted}$ are the rated or the nominal DC voltage and DC voltage as a result of the voltage sag respectively. For this simple formulation, $V_{dc,faulted}$ must be constant. T is the sag duration in seconds and R is the resistance of the load. Of course, more complex loads (e.g., time varying loads), and AC loads cannot be expressed in this

simple way. However, the V^2/R type formulation is often found in the literature as a measure of power irrespective of the load type. In fact, in communications work, the value $R=1\ \Omega$ is used thus making the formulation very simple.

The disturbance energy for different load types under different conditions of voltage sags is simulated for a six-pulse rectifier. The software for the simulation is PSpice. The simulation involves, setting up two rectifier systems, one to mimic a normal operation of the rectifier and the other the operation of the rectifier under a voltage sag event. Nominal three phase voltage system is applied to the rectifiers. After steady state has been achieved, the supply to one of the rectifiers is disturbed for a period of time. The energy delivered to the two rectifier systems during the disturbance duration is recorded. The difference in energy delivered to the two rectifier systems is the disturbance energy.

The disturbance energy for the different loads connected to the rectifier system shown in Figure 2.1 under different conditions of voltage sags are summarized for the cases shown in Table 2.1, and each case is discussed in detail below.

Table 2.1 Cases studied for a six-pulse diode bridge rectifier

Case	Conditions	
	AC supply	DC load
2.1	Balanced three phase	Pure resistive
2.2	Unbalanced (*VUF=0.5*)	Pure resistive
2.3	Balanced (50% sag)	Pure resistive
2.4	Unbalanced (phase-to-ground fault)	Pure resistive
2.5	Balanced (50% sag)	Inductive
2.6	Unbalanced (phase-to-ground fault)	Inductive
2.7	Balanced (50% sag)	Capacitive
2.8	Unbalanced (phase-to-ground fault)	Capacitive

a) Pure resistive load

The schematic circuit diagram for the six-pulse diode bridge rectifier connected with a pure resistive load is similar to the circuit diagram shown in Figure 2.1, the load being a pure resistor. The variation of disturbance energy with voltage sag duration for a pure resistive load is determined for the following types of voltage sags.

- **Voltage unbalance factor of 0.5 (Case 2.2)**

Voltage unbalance arises in a power distribution system due to incomplete transposition of transmission lines, unbalanced loads, open delta transformer connections, open fuses and failed three phase capacitor banks, just to mention a few. The aggravated effect of the presence of some amounts of unbalance in the line voltages will lead to

unproportional unbalance in the line currents [13]. Voltage unbalance factor is defined as the ratio of the magnitude of the negative sequence component of voltage in the three phase supply system to the magnitude of the corresponding positive sequence component.

Mathematically, voltage unbalance factor, VUF is given by

$$VUF = |V_-| / |V_+| .$$

In this expression, V_+ and V_- are the symmetrical components and

$$\begin{bmatrix} V_+ \\ V_- \\ Vo \end{bmatrix} = \frac{1}{3} \begin{bmatrix} a & a^2 & 1 \\ a^2 & a & 1 \\ 1 & 1 & 1 \end{bmatrix} \begin{bmatrix} V_{an} \\ V_{bn} \\ V_{cn} \end{bmatrix}$$

where $a = 1\angle 120°$. Under balanced conditions, $V_o = V_- = 0$. Under any condition, Parseval's theorem [4] requires

$$V_{RMS} = \sqrt{|V_-|^2 + |V_+|^2 + |V_o|^2} .$$

For a three phase six-pulse diode bridge rectifier, under unbalanced fundamental supply voltage conditions, harmonic currents result and therefore harmonic voltages at the rectifier result. These harmonics occur ideally only in positive and negative sequence. The presence of the negative sequence components in the fundamental supply voltage will lead to an overall reduction in the DC voltage at the load. The consequence of this voltage unbalance is the reduction of the power delivered to the load. The power reduction is the difference in power between the actual power delivered to the load as a result of the unbalance in the supply voltage and the power that would have been delivered in the absence of the voltage unbalance. The percentage power reduction is the ratio of the cited power reduction to the power delivered to the load in the absence of the voltage unbalance.

Figure 2.2 depicts variation of percentage power reduction for the six-pulse rectifier with pure resistive load. In this simulation the nominal RMS voltage is kept constant but the voltage unbalance factor is varied from zero to unity. Harmonic voltages in the AC supply are not considered. The variation of the disturbance energy with voltage sag disturbance duration for voltage sag of unbalance factor of 0.5 is shown in Figure 2.3. The supply voltage, *Vac* for this example analysis is 480 V RMS and the value of the DC circuit resistor *R* is 32.4 Ω.

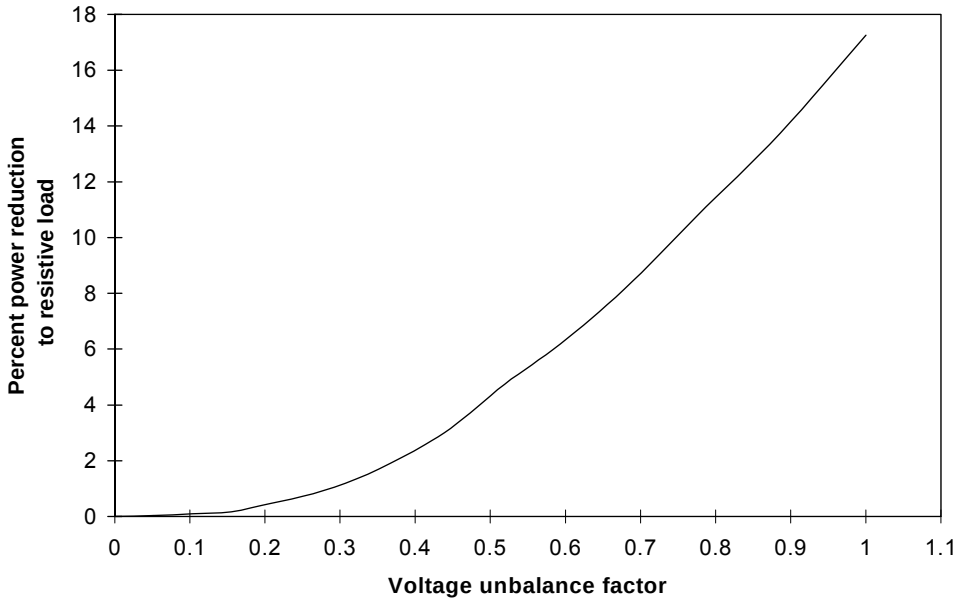

Figure 2.2 Percentage power reduction versus voltage unbalance factor for a six-pulse diode bridge rectifier with pure resistive load (Case 2.1)

From Figure 2.2 it is evident that an increase in voltage unbalance factor results in reduction in the power delivered to the load. The percentage reduction in power is approximately less than 4% when the voltage unbalance factor is less than 0.5. However, an increase in voltage unbalance factor beyond 0.5 leads to a drastic reduction in the

power delivered to the load. Inspection of Figure 2.3 reveals that the disturbance energy increases linearly with the time duration of the voltage sag for the voltage unbalance factor of 0.5.

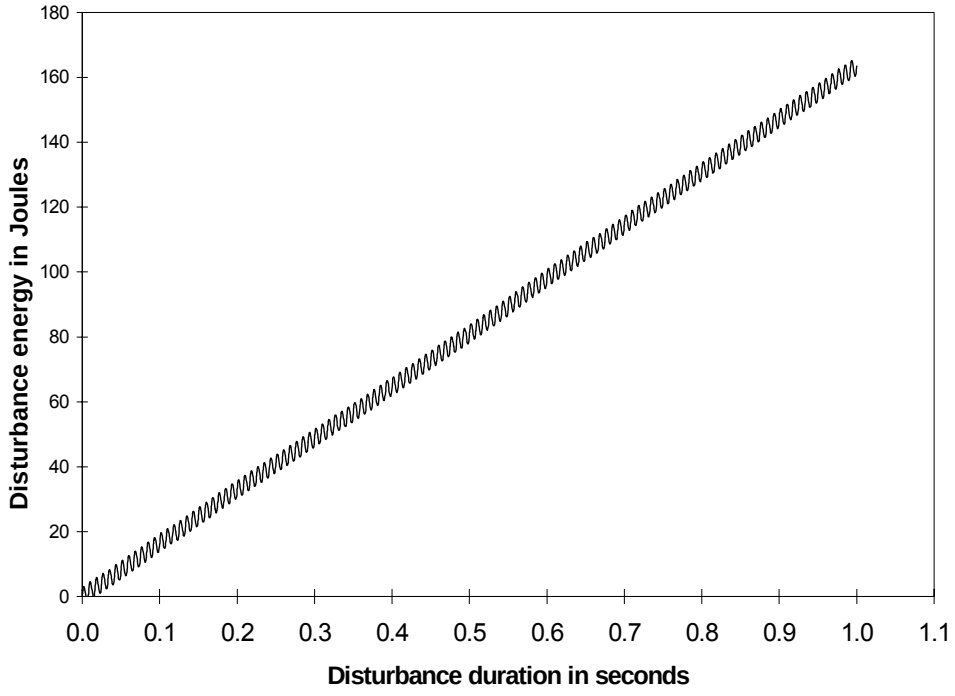

Figure 2.3 Disturbance energy for six-pulse diode bridge rectifier with pure resistive load (voltage sag with unbalance factor of 0.5) (Case 2.2)

- **Three phase 50% voltage sag (Case 2.3)**

Using the same example circuit, with voltage sag of 50% applied to all the three phases of the supply voltage and the simulation carried out, the variation of the disturbance energy with the voltage sag duration is depicted in Figure 2.4 for a pure resistive load ($R_{DC}=32.4\ \Omega$). Three phase voltage sag usually occurs, for example, when

a large induction motor connected to the point of common coupling is started. The disturbance energy is a simple linear function of disturbance duration in this case.

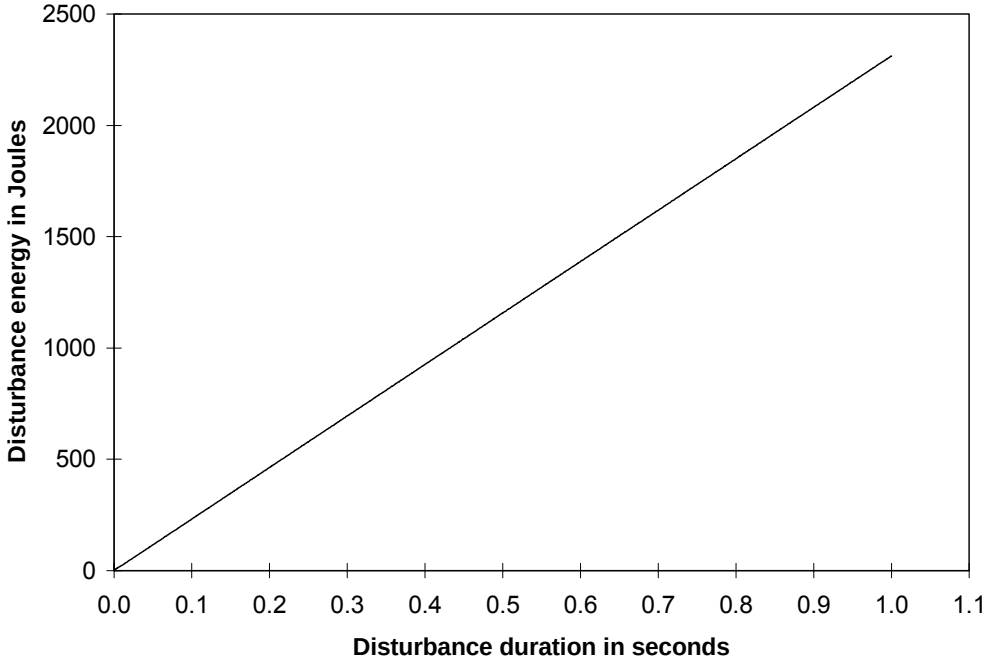

Figure 2.4 Disturbance energy for six-pulse diode bridge rectifier with pure resistive load (50% three phase voltage sag, *Vac=480 V* RMS) (Case 2.3)

- **Single phase-to-ground fault (Case 2.4)**

The large majority of faults on a utility system are single phase-to-ground faults. Single phase-to-ground faults are unbalanced and usually result from weather conditions such as lightning. When a single phase-to-ground fault occurs, the voltage on the faulted phase goes to zero at the fault location. This is simulated by connecting the phase 'a' of the three phase supply to the six-pulse diode bridge rectifier to ground after steady state

has been achieved. The disturbance energy versus the voltage sag duration is shown in Figure 2.5.

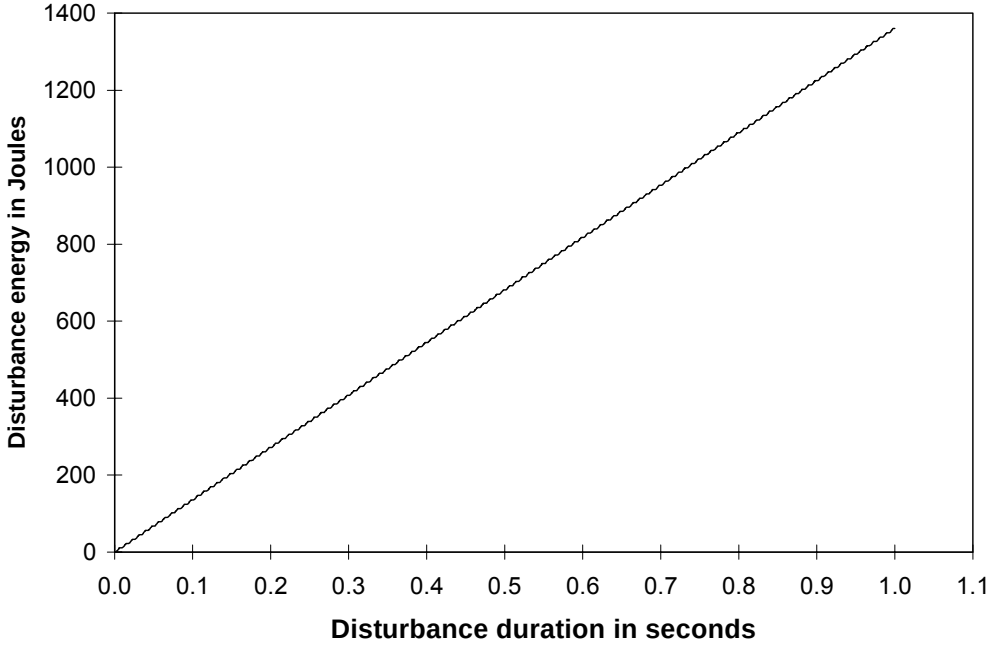

Figure 2.5 Disturbance energy for six-pulse diode bridge rectifier with pure resistive load (Phase 'a'-to-ground fault, V_{ac}=*480 V* RMS) (Case 2.4)

b) Inductive load

In this study an inductive load in the DC side of a six-pulse rectifier is considered. The intent is to evaluate the effect of voltage sags on the inductive load by calculating the disturbance energy through simulation. The schematic circuit diagram for the simulation is similar to the circuit shown in Figure 2.1. The inductive load consists of a 64.9 H inductor in series with a 32.4 Ω resistor. The size of the inductor selected ensures that the load current is constant. Two simulations are performed: a balanced three phase voltage sag and an unbalanced phase 'a'-to-ground fault. Figure 2.6 depicts the

disturbance energy for six-pulse diode bridge with an inductive load, 50% balanced voltage sag. The disturbance energy for the case of phase 'a'-to-ground fault for an inductive load connected to the six-pulse diode bridge is shown in Figure 2.7.

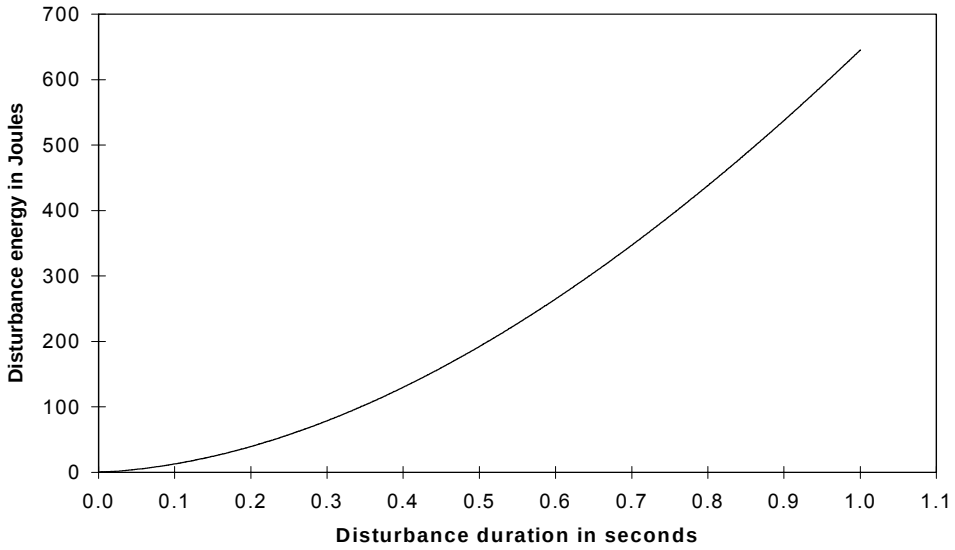

Figure 2.6 Disturbance energy for six-pulse diode bridge rectifier with inductive load (50% voltage sag, V_{ac}=*480 V* RMS) (Case 2.5)

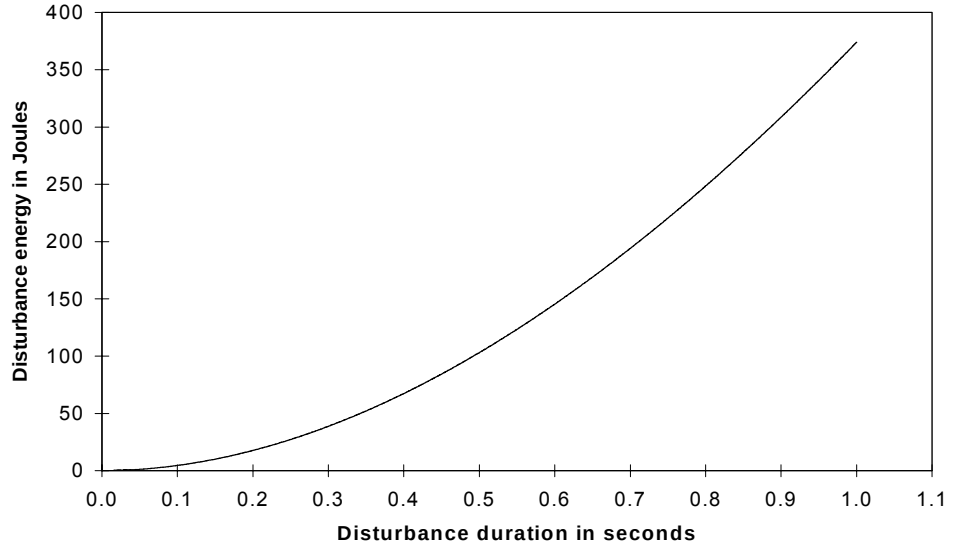

Figure 2.7 Disturbance energy for six-pulse diode bridge rectifier with inductive load (Phase 'a'-to-ground fault, V_{ac}=*480 V* RMS) (Case 2.6)

c) Capacitive load

Consider the case of capacitive load in the DC side of the six-pulse rectifier as depicted in Figure 2.8. The capacitive load comprises of a 10 mF capacitor in parallel with a 32.4 Ω resistor. The intent, the method and the approach of the simulation are similar to the one employed in the case of the inductive load. Figures 2.9 and 2.10 are the disturbance energies for six-pulse diode bridge with capacitive load for the cases of 50% balanced voltage sag and unbalanced phase 'a'-to-ground fault respectively.

From Figures 2.9 and 2.10 it can be observed that the disturbance energy varies linearly with the disturbance duration for both the cases of 50% balanced voltage sag and unbalanced phase 'a'-to-ground fault. However the impact of the disturbance is severe when the fault under consideration is a 50% balanced voltage sag.

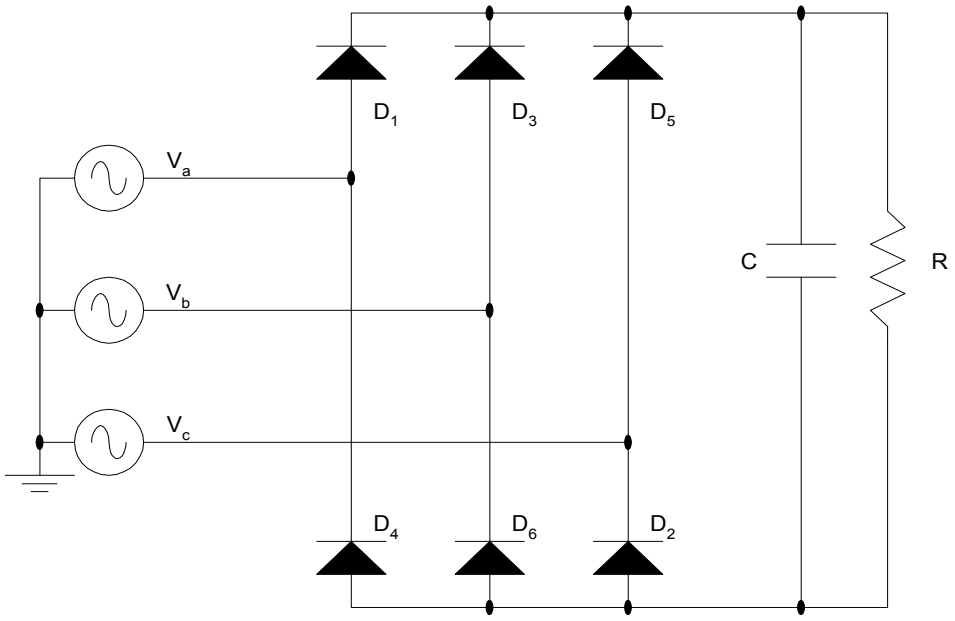

Figure 2.8 Schematic diagram for six-pulse rectifier system with capacitive load

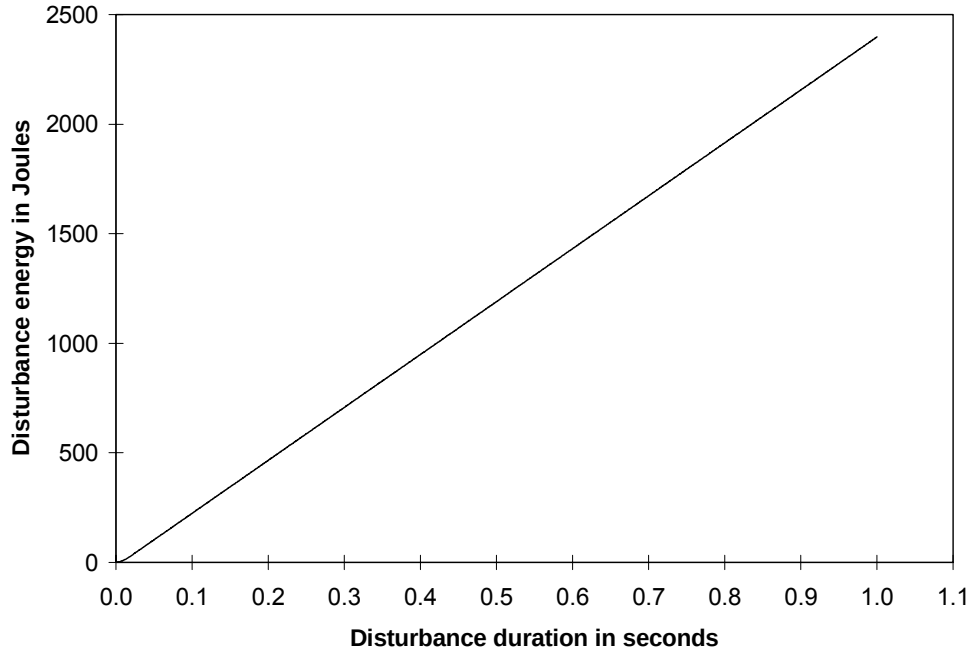

Figure 2.9 Disturbance energy for six-pulse diode bridge rectifier with capacitive load (50% voltage sag, V_{ac}=*480 V* RMS) (Case 2.7)

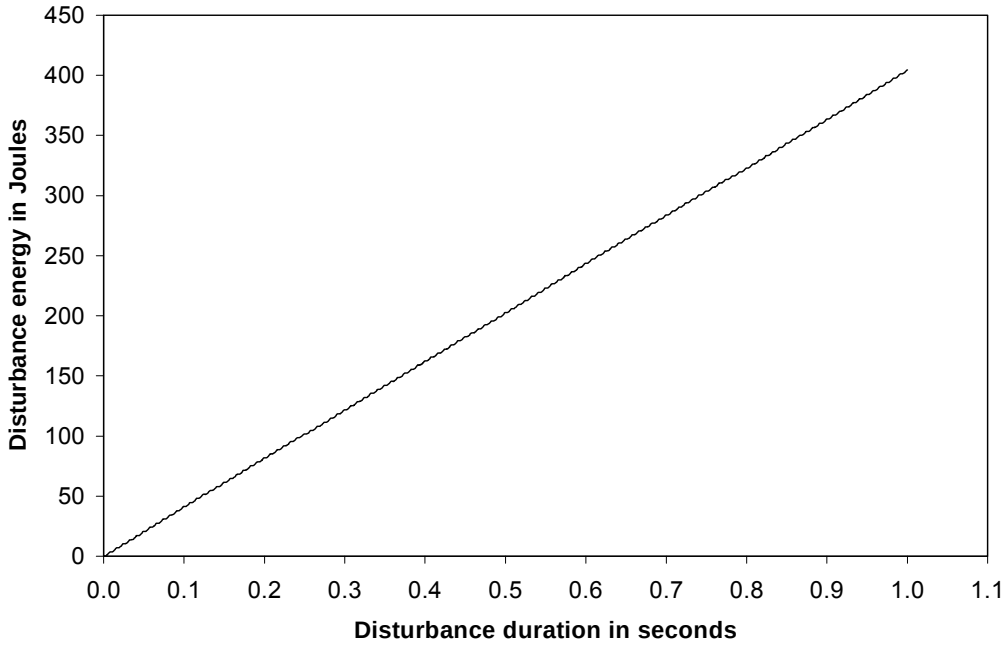

Figure (2.10) Disturbance energy for six-pulse diode bridge rectifier with capacitive load (Phase 'a'-to-ground fault, V_{ac}=*480 V* RMS) (Case 2.8)

2.5 Disturbance energy and CBEMA curve

In the previous sections the variation of disturbance energy with voltage sags for different loads were illustrated. In this section, it is intended to find the correlation if any between the disturbance energy and the CBEMA curve. That is to determine whether CBEMA is based on disturbance energy concept.

The approach involves calculating disturbance energies for six-pulse diode bridge rectifier with pure resistive and inductive loads for different three phase voltage sags through simulation. The simulation is done for a time duration that corresponds to the threshold sag duration time for the different sag depths on the CBEMA curve. Table 2.2 depicts the threshold disturbance energies for different three phase voltage sag depths for six-pulse diode bridge rectifier with resistive and inductive loads.

Inspection of Table 2.2 reveals that the threshold disturbance energy for both the resistive and the inductive loads increase with reduction in the percent voltage sag. However, one would have expected the threshold disturbance energy to remain constant with reduction in the percent voltage sag for the stated threshold disturbance durations if power acceptability curves are to be considered as loci of constant energy. From Table 2.2, CBEMA curve may not be considered, as locus of constant energy and it is therefore not based on energy.

Table 2.2 Threshold disturbance energy for six-pulse diode bridge rectifier with resistive and inductive loads (balanced three phase sag)

Voltage sag (percent)	Disturbance duration (seconds)	Threshold disturbance energy (Joules)	
		Resistive load (R=32.4 Ω)	Inductive load (R=32.4 Ω, L =64.9 H)
-20	1.730	7992.7	4621.6
-25	0.669	2472.7	663.9
-30	0.315	1416.4	239.1
-35	0.213	720.9	66.6
-40	0.100	437.7	25.7
-45	0.057	188.2	5.02
-50	0.042	130.7	2.55

2.6 Summary of the concept of disturbance energy

The concept of disturbance energy has been analyzed, simulated and illustrated using a three phase line commutated rectifier. It is evident from the simulation results that disturbance energy is a function of the disturbance duration for all the different load types considered in the DC circuit of the rectifier.

The following are the salient points that resulted from the simulation and verification of the concept of disturbance energy:

- The disturbance energy increases with the duration of the sag event. The increase however depends of the nature of the sag and the load in the DC circuit of the rectifier. In particular it is realized that for a given sag event and sag duration the disturbance energy is higher when the load in the DC circuit of the rectifier is

capacitive or pure resistive in nature. Inductive loads in the DC circuit of the rectifier generally resulted in comparatively lower disturbance energies for the sag events considered. It is worthwhile to note that 50% three phase supply voltage sag has greater impact than the corresponding phase 'a' to ground fault for any of the load types considered.

- The relationship between voltage unbalance factor and the percentage power loss to the rectifier load is demonstrated. It is realized that when the supply voltage is highly unbalanced ($VUF \geq 0.5$) the percentage power loss to the load becomes excessively high.
- It is revealed that the CBEMA curve is not based on the concept of disturbance energy.

Chapter 3

Design of power acceptability curves

3.1 Introduction

The design of power acceptability curves relates to whether the distributed power can be utilized or not. In other words, the distribution power should be considered acceptable if the industrial process served is operative. Thus, the ultimate criterion of power acceptability relates to the operational status of the industrial process. This criterion depends on the nature of the load. For example, simple incandescent lighting loads may have a very loose criterion for acceptability, while certain sensitive computer controls may have a much more restrictive criterion. The difficulty in the selection of a single criterion is confounded by the many possible load types.

In this chapter, the concept of a power quality standard is introduced and it is used to construct power acceptability curves for any load type (including the single and three phase cases) for which the model of the load is known. The majority of this chapter was also reported in the author's work in [19].

3.2 The concept of a power quality standard

Power acceptability curves are aides in the determination of the acceptability of supply voltage to a load or an industrial process. There is no single power acceptability curve applicable to all loads. However different curves may be designed to capture different load types and power quality standards. The term 'power quality standard' or 'standard' in short, used in this context refers to the ultimate criterion upon which a decision of acceptability of supply is made. For an illustration, consider the rectifier load

type depicted in Figure 3.1. Voltage sags occurring due to faults in the transmission, subtransmission, and primary distribution system appear as low voltage condition at V_{ac} depicted in Figure 3.1. If the sag is of short duration and shallow in depth, the ultimate industrial process 'rides through' the disturbance. This means that although V_{ac} is depressed, V_{dc} does not experience a sufficient disturbance to affect the industrial process.

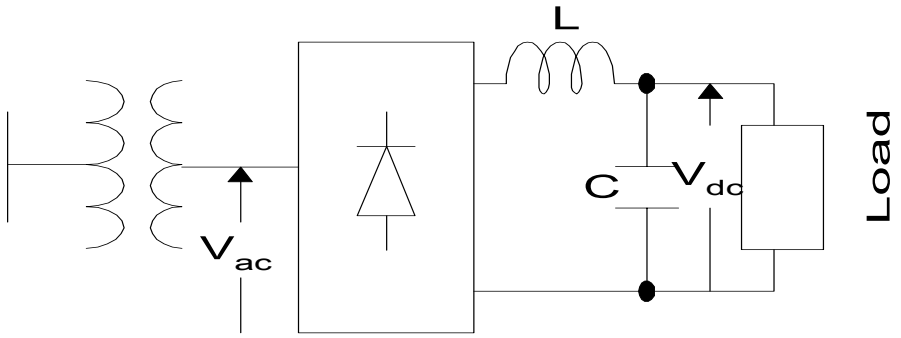

Figure 3.1 A rectifier load

The concept of power quality standard (voltage standard in this case) is introduced at this point: a voltage standard is a criterion for power acceptability based on a minimum acceptable DC voltage at the output of a rectifier below which proper operation of the load is disrupted. As an example, a voltage standard of 87% for the rectifier system means that if the V_{dc} drops below 87% of the rated voltage, the load will be lost, and the distribution power will be deemed to be unacceptable. The use of the term 'standard' is however, not meant to imply industry wide standard such as IEEE standards.

Different loads and industrial processes have different standards. For example, a rotating load may have a *speed standard* based on a minimum acceptable shaft speed below which the industrial process is lost. An electromechanical relay may have a *force*

standard that quantifies the force required to hold a relay armature in a given closed position. A heating process may have a *temperature standard*. Each of these standards entails an ultimate quantity that is related to the AC distribution bus voltage by a differential equation. The time domain solution of the differential equation yields the ΔV - T plane locus of the acceptable and unacceptable regions. Thus the concept of a power quality standard may be used to construct a power acceptability curve for any load type.

3.3 'Derivation' of the CBEMA curve

The CBEMA curve was derived from experimental and historical data taken from mainframe computers. The best scientific interpretation of the CBEMA curve can be given in terms of a voltage standard applied to the DC bus voltage of a rectifier load.

Consider the case of either a single phase full wave bridge rectifier or the three phase bridge counterpart. Let the load on the DC side be an *RLC* load. If the DC bus voltage under faulted condition is plotted as a function of the sag duration, the resulting curve is depicted in Figure 3.2. From Figure 3.2 the locus of V_{dc} could be represented as a double exponential in the form,

$$V_{dc}(t) = A + Be^{-bt} + Ce^{-ct}. \tag{3.1}$$

Parameter A is the ultimate ($t \to \infty$) voltage, V_{end}, of the rectifier output. For the single phase case, and for the balanced three phase case, A is simply the depth of the AC bus voltage sag. For more complex cases, e.g. unbalanced sags, parameter A can similarly be identified as the ultimate DC circuit voltage if the sag were to persist indefinitely (this is readily calculable by steady state analysis of the given sag condition and the rectifier type).

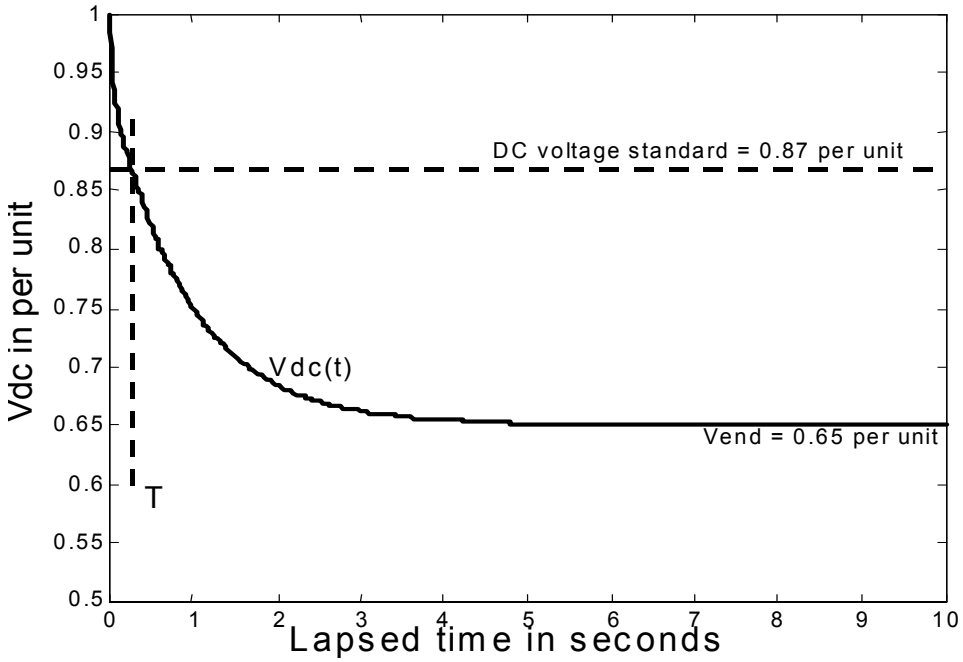

Figure 3.2 Locus of $V_{dc}(t)$ under fault conditions (at $t = 0$) for a single phase bridge rectifier

The method employed in finding the constants *B* and *C*, and time constants *b, c* in Equation (3.1) involves selecting three points on the CBEMA curve and applying Newton's method (shown in Appendix A). Table 3.1 depicts points on the CBEMA curve.

Table 3.1 Extracted points on CBEMA curve

Time (seconds)	Percent voltage sag
0.00833*	-100
0.01	-91.4
0.02	-66.4
0.03	-57.6
0.04	-53.3
0.05	-48.8
0.06	-44.4
0.07	-43.3
0.08	-42.1
0.09	-41.5
0.1*	-40.0
0.2	-35.6
0.3	-31.1
0.4	-28.9
0.5	-26.5
0.6	-25.6
0.7	-24.4
0.8	-23.7
0.9	-23.3
1*	-23.0
2	-17.8
3	-16.9
* Points used in deriving the formula for the CBEMA curve	

The selection of the three points from the CBEMA curve identifies the *RLC* filter combination used in the rectifier types considered in the original CBEMA tests. By

substituting the output of the Newton's method (that is the values of the constants B, C, b and c), one finds,

$$V_{dc}(t)=V_{end}+0.288e^{-1.06t}+(0.712-V_{end})e^{-23.7t}. \quad (3.2)$$

For the CBEMA curve, let the voltage standard be $V_{dc} \geq 0.87$. Then the V_{dc} excursion becomes unacceptable at T when $V_{dc}= 0.87$ in Equation (3.2). The solution of V_{end} in terms of $t=T$ Equation (3.2) gives

$$V_{end} = \frac{0.87 - 0.288\ e^{-1.06\ T} - 0.712\ e^{-23.7\ T}}{1 - e^{-23.7\ T}}.$$

This is the 'formula' for the undervoltage limb of the CBEMA curve (V_{end} in per unit, T in seconds).

3.4 The unbalanced three phase case

Balanced voltage sag events in three phase systems can be treated effectively as a single phase equivalent. The original CBEMA curve is utilized to address this case. However, most voltage sags are unbalanced. The voltage sags are as a result of unbalanced faults such as phase-to-ground, phase-to-phase-to-ground, and phase-to-phase faults. Perhaps the most common fault type is the phase-to-ground fault in which one of the phase voltages is depressed.

All the highlighted causes of voltage sag events will have to be considered if one is to develop a meaningful power acceptability curve for three phase systems. However, developing a single power acceptability curve to capture all these possible scenarios is nearly impossible. The approach taken here is one of modeling several fault types in conjunction with a dynamic load model in order to obtain a power acceptability curve.

The ultimate 'standard' is often a DC voltage although speed or other standards may be used as the load process warrants.

Figure 3.3 shows a power acceptability curve for a three phase rectifier. The case considered here is that of a phase ‘a’ to ground fault using an 87% V_{dc} voltage standard. The procedure for the development of the power acceptability curve is similar to the one employed in deriving Equation (3.2). The unbalanced fault for the three phase rectifier is analyzed simply, and $V_{dc}(t)$ in this case is given as

$$V_{dc}(t) = V_{end} + 0.159e^{-0.158t} + (0.841-V_{end})e^{-4.63t} . \quad (3.3)$$

In Equation (3.3), the time constants were obtained using an *LC* filter on the DC side of a three phase, six-pulse bridge rectifier. The values of the *LC* were chosen to agree with the filter design used in the single phase case mentioned in conection with the derivation of Equation (3.2). That is, the CBEMA curve was found to correspond to the single phase rectifier case plus filter *F*. If filter *F* is used as a filter in the *three phase* case, Equation (3.3) results. For a voltage standard of

$$V_{dc} \geq 0.87$$

when substituted into Equation (3.3) gives a formula for the power acceptability curve shown in Figure 3.3 as

$$V_{end} = \frac{0.87 - 0.159\, e^{-0.158\,T} - 0.841\, e^{-4.63\,T}}{1 - e^{-4.63\,T}} .$$

Power acceptability curve for the case of three phase rectifier with phase-to-phase-to-ground is shown in Appendix B.

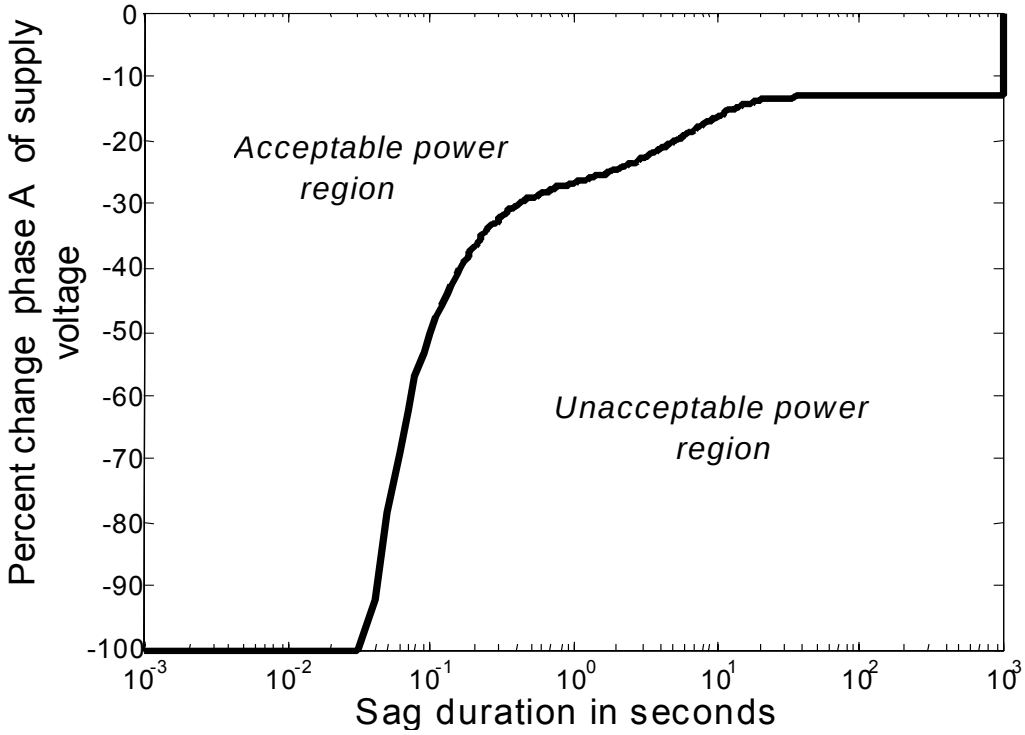

Figure 3.3 Power acceptability curve for a three phase rectifier load with a phase-ground fault at phase 'a', 87% V_{dc} voltage standard

3.5 The speed standard

An important implication of the use of the concept of 'standards' to design power acceptability curves is that many different industrial processes may be represented. A rotating load such as induction motor may be thought of to have a standard based on a minimum acceptable shaft speed, *speed standard*, below which the operation of the motor or the industrial process is unacceptable.

The use of the speed standard implies that the industrial process is irreparably disrupted when the shaft speed of the motor drops below a threshold (e.g., 95% the rated speed). The problem is complex because of the following issues:

- The machine must be modeled under balanced or unbalanced conditions as appropriate.
- The variation of shaft torque should be modeled. If the threshold shaft speed is near the rating, the load torque model is not crucial because the shaft torque is nearly fixed.
- Different machine types and drives may have to be considered.

In this thesis a balanced model of the induction motor is employed for different variation of load torques but for a speed standard of 95% the rated motor speed.

3.6 Induction motor load representation

For induction motor loads served directly from AC bus, Figure 3.4 applies. The steady state equivalent circuit from which machine performance can be calculated is depicted in Figure 3.5. From Figure 3.5, the following electrical and mechanical equations for the induction motor load can be derived.

a) The slip of the motor, s is given as

$$s = \frac{\omega_s - \omega}{\omega_s} \tag{3.4}$$

where ω_s and ω are the synchronous and shaft speeds of the machine respectively.

b) The shaft torque, T_e is defined in terms of the machine parameter r_2 as

$$T_e = 3\frac{I_2^{\,2} r_2}{s\omega_s} \tag{3.5}$$

where, I_2 is the current flowing the rotor winding at steady state.

c) The differential equation relating the shaft torque and the speed is

$$T_e = J\dot{\omega} + B\omega + T_L . \tag{3.6}$$

In this expression, T_L is the load torque, $B\omega$ models viscous friction and J is the shaft moment of inertia. The solution of the differential equation in Equation (3.6) can be approximated for small values of t assuming that viscous friction is negligibly small as

$$\omega(t) = \omega_0 + K\Delta t \tag{3.7}$$

where, K is a constant that depends on the relative magnitudes of T_e, T_L and J.

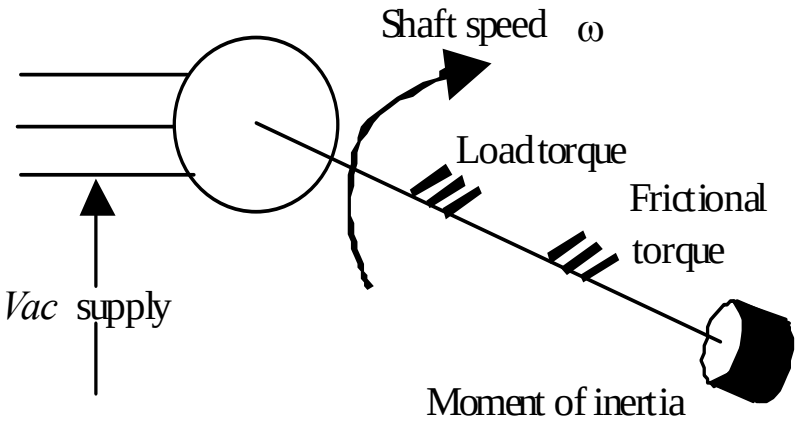

Figure 3.4 Induction machine served from an AC bus

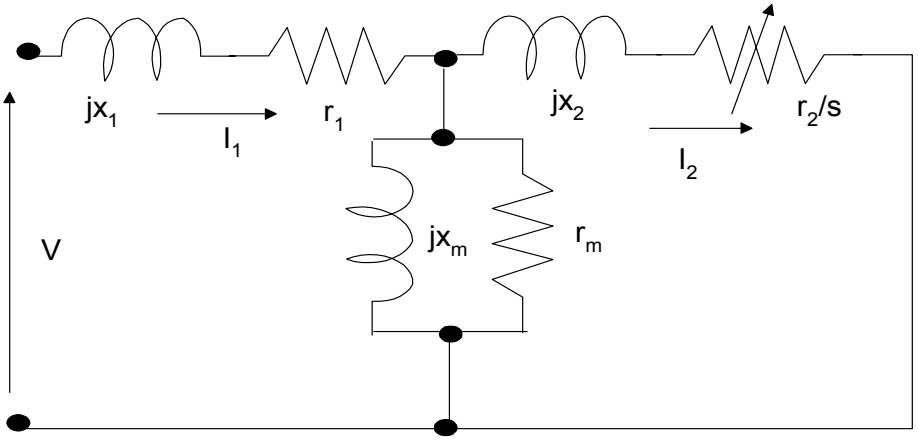

Figure 3.5 Elementary positive sequence induction machine model

3.7 Pseudocode for the design of a power acceptability curve for an induction motor load

With an access to the induction motor parameters, the family of curves corresponding to various sag depths as shown in Figure 3.6 can be obtained through simulation. The load torque is assumed to be proportional to the shaft speed of the induction motor. The pseudocode for the simulation is:

Begin

Enter the machine parameters

Initialize $t = 0$, $\omega = \omega_{rated}$

Calculate slip S, torques T_e *and* T_L

Calculate shaft speed $\omega(t) = \omega_0 + K\Delta t$

While ($T_e < T_L$)

Calculate slip S, torques T_e *and* T_L

Calculate shaft speed $\omega(t) = \omega_0 + K\Delta t$

End while

Plot $\omega(t)$

The complete MATLAB code for the simulation is shown in Appendix C.

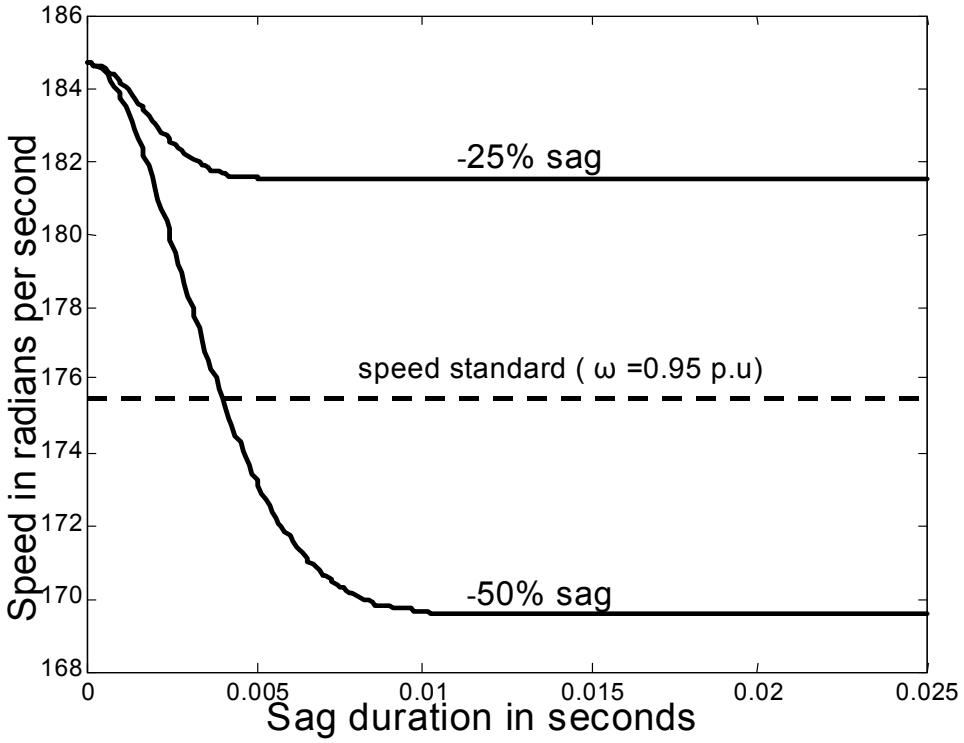

Figure 3.6 Family of curves for the speed of a 4 pole, 60 Hz, 2% slip, induction machine for different sag depths

From Figure 3.6, the locus of *Vac* could be represented as a double exponential in the form,

$$Vac(t)=A + Be^{-bt} + Ce^{-ct}. \tag{3.8}$$

Parameter A is the ultimate ($t\rightarrow\infty$) voltage (i.e., V_{end}) at the input of the induction motor if the fault were to persist indefinitely. If the speed standard is $\omega\geq 0.95$ per unit, the crossing points of curves in Figure 3.6 with the speed standard are used to determine the values of the constants *B, C, b* and *c* in Equation (3.8) with the application of Newton's method. The equation of the power acceptability curve is given by approximately,

$$V_{end} = \frac{0.575-0.425e^{-1800T}-0.575e^{-2.931T}}{1-e^{-2.931T}}.$$

The power acceptability curve under the stated conditions for an induction motor load is shown in Figure 3.7.

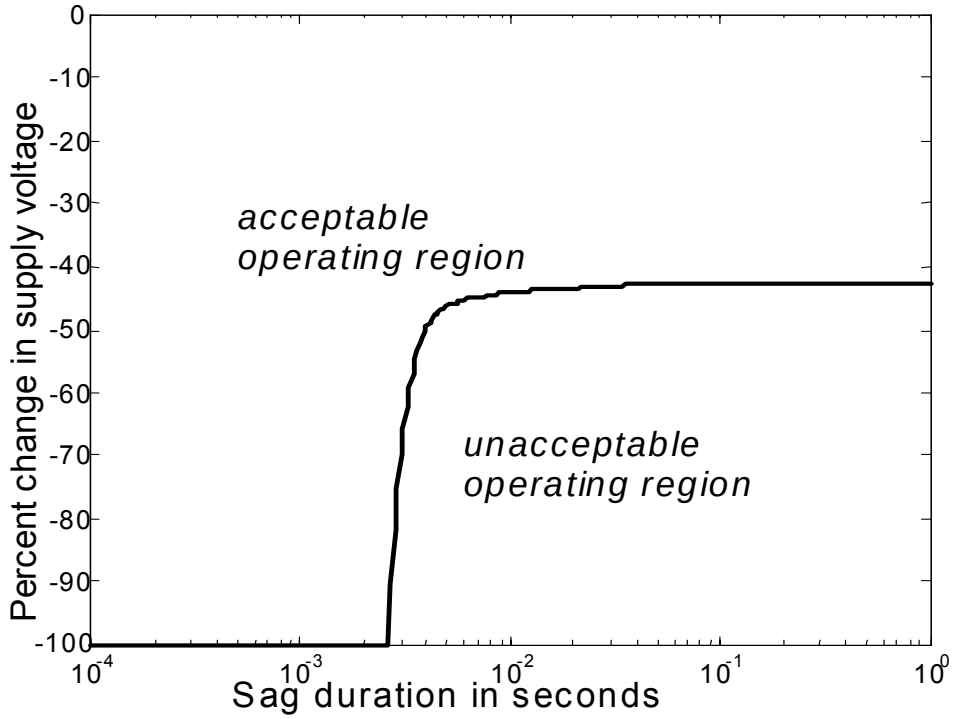

Figure 3.7 A power acceptability curve (undervoltage region) for an induction motor load, speed standard $\omega > 0.95$ per unit, load torque assumed proportional to shaft speed

3.8 Power acceptability curves for other induction motor load types

Induction motors are employed in driving different types of loads in industry and commercial establishments. The torque characteristics of these loads vary significantly, from one where the load torque is constant independent of shaft speed to one where the load torque is proportional to the cube of the shaft speed. The question that one may ask is, can a single power acceptability curve be applied to any of these possible industrial and commercial loads? Figure 3.8 depicts the power acceptability curve for the induction

motor load, load torque assumed to be constant. The development of this curve is similar to that shown in Figure 3.7 with the exception that the load torque is constant.

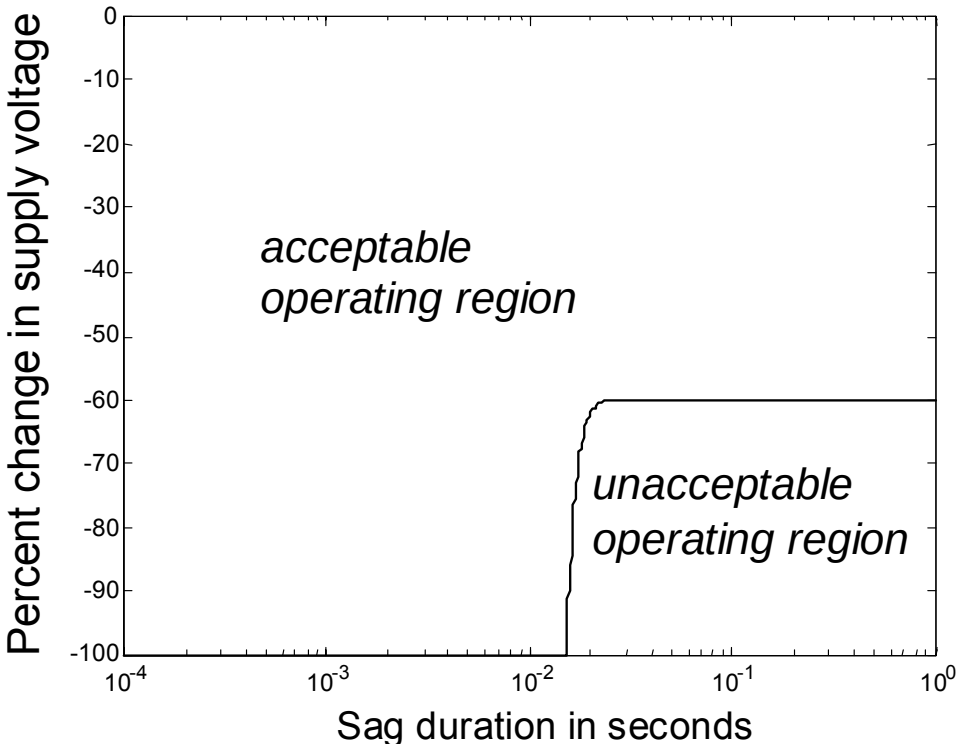

Figure 3.8 A power acceptability curve (undervoltage region) for an induction motor load, speed standard $\omega > 0.95$ per unit, load torque assumed to be constant

The case of induction motor driving a load whose torque characteristics vary as the square of the motor shaft speed is shown in Figure 3.9. It could be observed from Figures 3.7, 3.8 and 3.9 that the load driven by the induction motor plays a critical role as to how susceptible the machine will be to voltage sags. Whereas an induction motor driving a constant torque load can withstand voltage sag of approximately 60% indefinitely without tripping, the induction motor driving a load with torque proportional to the shaft speed can only withstand voltage sag of approximately 42% indefinitely.

Thus, one needs to have an idea of the driven load torque characteristics in order to make an informed decision as to which power acceptability curve to apply. If the induction motor drives multiple loads of different torque characteristics, one might apply a power acceptability curve with narrowest acceptable operating region.

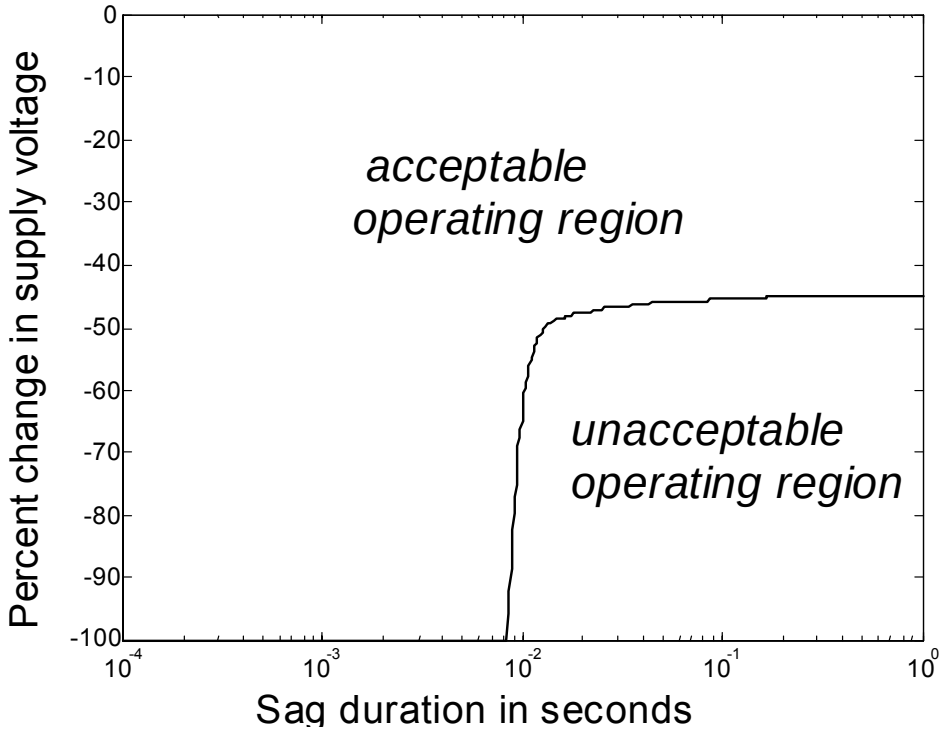

Figure 3.9 A power acceptability curve (undervoltage region) for an induction motor load, speed standard $\omega > 0.95$ per unit, load torque assumed proportional to the square of the shaft speed

3.9 The force standard

Power line disturbances such as voltage sags may lead to disruption of continuous processing industries. The industrial equipment responds in different ways to the sag event. In some cases, the best solution is to protect the equipment from voltage sags with the use of voltage restorers such as dynamic voltage restorer. In other cases, it may be economical to protect the susceptible equipment by isolating it from the supply line. AC contactors are usually employed in the latter option to make and unmake contacts between the industrial equipment and electrical system for power or control purposes. The question that one may ask is, are these contactors capable of riding through voltage sags?

In many industrial processes, rotating machines are controlled by AC contactors. While the rotating machines often have inertia to ride through voltage sag disturbances, contactors have been shown to be particularly more susceptible to voltage sags [21]. An AC contactor can therefore be considered to require a minimum magnetic holding force, *force standard,* to maintain the movable contact in a closed position.

In this work, a force standard of 80% the rated magnetic holding force is used to design power acceptability curves for electromechanical relays such as AC contactor under voltage sags.

3.10 Modeling of AC contactor

The AC contactor used in the design of the power acceptability curve is as shown in Figure 3.10. As depicted in Figure 3.10, the contactor coil is modeled as a resistance R in series with an inductance L. The contactor receives its supply from an AC source and the coil provides a magnetic force, which offsets the tension in the spring and ultimately

causes the electrical contacts to make. The behavior of the contactor under voltage sags can be understood if one considers the impact of the sags on the current flowing through the coil. The magnetic force attracting and holding the movable electrical contact in position varies as the square of the coil current. The magnetic force oscillates and becomes zero twice every cycle. The magnetic force thus falls below the minimum holding force required to keep the movable contact in a closed position for a small interval of time in each cycle, however the mechanical design and the inertial of contactor allows it to remain in the closed position. The electrical contacts of the contactor will therefore remain intact during normal operation. The average effective magnetic force is one-half of the maximum force. During voltage sags the effective magnetic force will decrease and the contactor will disengage depending on the depth, the duration of the sag and the point-on-wave where the sag occurs.

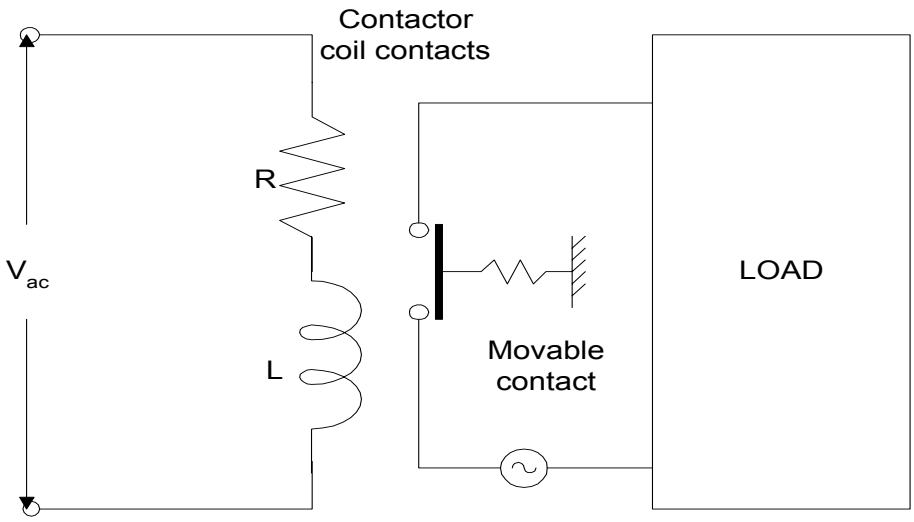

Figure 3.10 Simplified AC contactor model

3.11 Design of power acceptability curve for AC contactors

The design process involves simulating a simplified equivalent circuit of the AC contactor, which consists of a resistor *R* in series with an inductor *L*, connected to an AC supply using Pspice. The values of *R* and *L* were selected such that the ratio of the reactance to the resistance of the contactor coil is comparable with measurement taken from a typical 60 Hz, 120 V AC contactor. With the assumption that the average effective magnetic force is proportional to the average of the square of the current through the contactor coil, the average effective magnetic force required to hold the movable contactor in a closed position at the rated voltage is estimated. Different reduced voltages are applied to the AC contactor at steady state and the times required for the average effective magnetic holding force to fall to 80% of the rated value (i.e. the force standard) calculated. The simulation is done for the case where the sag event occur when the instantaneous value of the supply voltage is zero and the one at which the voltage is at its peak value. The idea is to find out the impact of the point-on-wave where the sag event occurs on the performance of the AC contactor.

A double exponential equation model is developed for the locus of the different voltage sags and the times required for the magnetic holding force to reach the force standard of 80%. The equation describing the undervoltage region of an AC contactor under voltage sag with sag event occurring at the point-on-wave where the instantaneous value of the supply voltage is zero is obtained to be approximately

$$V_{end} = \frac{0.9 - 0.1e^{-711.6T} - 0.9e^{-0.0272T}}{1 - e^{-0.0272T}}. \qquad (3.9)$$

The method and the approach used in obtaining Equation (3.9) are similar to the one used in deriving Equation (3.2). Figure 3.11 is a graphical representation of Equation (3.9).

Figure 3.11 depicts power acceptability curve for an AC contactor with point-on-wave where sag event occurred being zero instantaneous voltage and force standard of 80%.

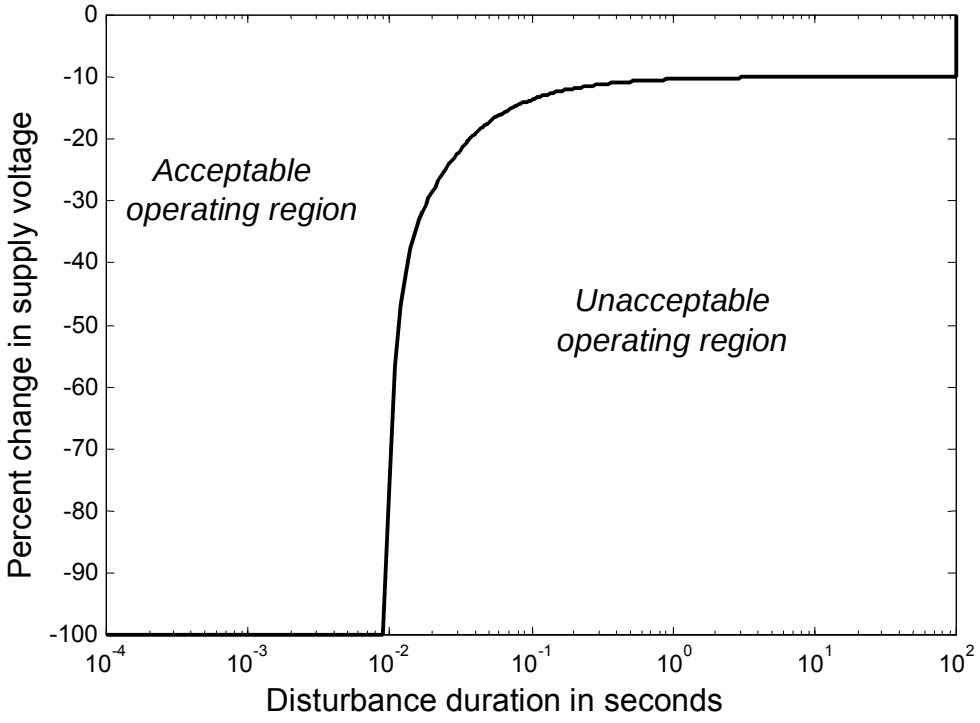

Figure 3.11 A power acceptability curve (undervoltage region) for an AC contactor (point-on-wave where sag occurred= zero instantaneous voltage; force standard= 80%)

For an AC contactor undervoltage sags with point on wave where sag event occurred being peak of instantaneous voltage and force standard of 80%, Figure 3.12 results. From Figure 3.11 and Figure 3.12 it is evident that point-on-wave where sag event occurs plays a role as to the ride-through capability of an AC contactor undervoltage sag. The acceptable operating region of an AC contactor undervoltage sag where the sag event occurs at zero instantaneous voltage is slightly wider than for the case where the sag event occurs at peak instantaneous voltage. However, in both cases a sag event of 10% the rated voltage can be sustained indefinitely.

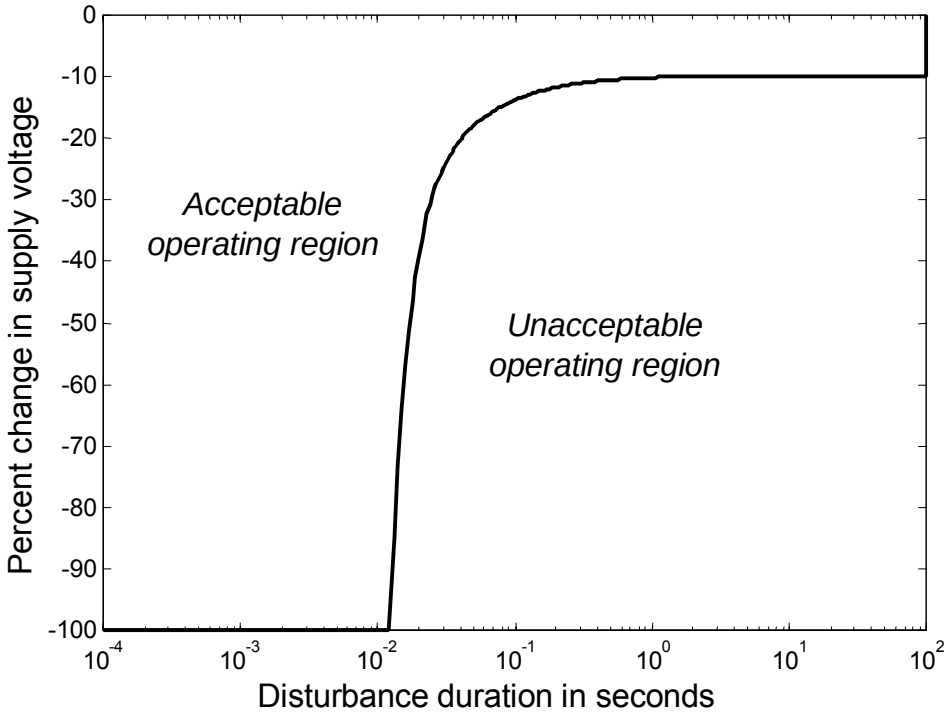

Figure 3.12 A power acceptability curve (undervoltage region) for an AC contactor (point-on-wave where sag occurred= peak instantaneous voltage; force standard= 80%)

3.12 Construction of power acceptability curves

Consider a rectifier system operating under a faulted AC voltage supply. Figure 3.13 depicts the DC voltage of the rectifier under the condition of faulting the AC voltage supply at time $t = 0$. The equation of this DC voltage response is of the form

$$V_{dc}(t) = V_{end} + Ae^{-at} + Be^{-bt}. \tag{3.10}$$

At time $t = 0$,

$$B = 1 - V_{end} - A.$$

Also, let $t = T$ be the time to reach the threshold value of the DC bus voltage, V_T. These, when substituted into Equation (3.10) result in

$$V_T = V_{end} + Ae^{-aT} + (1 - V_{end} - A)e^{-bT}. \tag{3.11}$$

The voltage sag, ΔV is given as

$$\Delta V = V_{end} - 1. \tag{3.12}$$

Combining Equations (3.11) and (3.12), the voltage sag, ΔV is obtained as

$$\Delta V = \frac{V_T + A\left(e^{-aT} - e^{-bT}\right) - 1}{1 - e^{-bT}}. \tag{3.13}$$

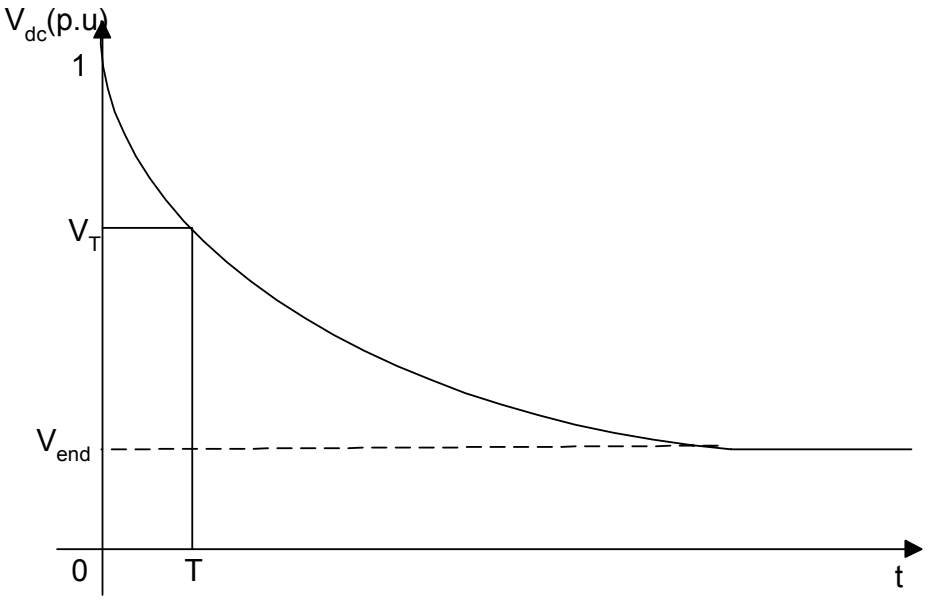

Figure 3.13 Rectifier load on an AC system, fault occurs at $t = 0$, DC voltage depicted

Equation (3.13) is the equation of the ΔV - T locus of the undervoltage limb of a CBEMA-like power acceptability curve. To identify parameters V_T, A, a, and b, note the following: let T_x be the value of the disturbance time T for which a total outage (that is, ΔV = -1.0 per unit) may be tolerated. Then,

$$-1 = \frac{V_T + A\left(e^{-aT_x} - e^{-bT_x}\right) - 1}{1 - e^{-bT_x}}.$$

Eliminating parameter A gives,

$$\Delta V = \frac{V_T + \frac{e^{-bT_x} - V_T}{e^{-bT_x} - e^{-aT_x}}\left(e^{-bT} - e^{-aT_x}\right) - 1}{1 - e^{-bT}}. \qquad (3.14)$$

Equation (3.14) is the equation of a power acceptability undervoltage curve given the DC standard V_T and the two filter time constants *a, b.*

3.13 Power acceptability for the case of multiple loads

In practical cases, distribution circuits serve many loads. Each load potentially has its own standard of power acceptability as well as its own dynamic characteristics. A conservative approach is to define the overall acceptability region as the intersection of the individual acceptable regions.

As an example, consider three separate rectifier loads, each can tolerate total AC voltage outage for 1/120 second each with 87% V_{dc} voltage standard. If three representative sets of time constants are used in Equation (3.14), Figure 3.14 results. The intersection of the three acceptable regions is shown as the shaded area in Figure 3.14.

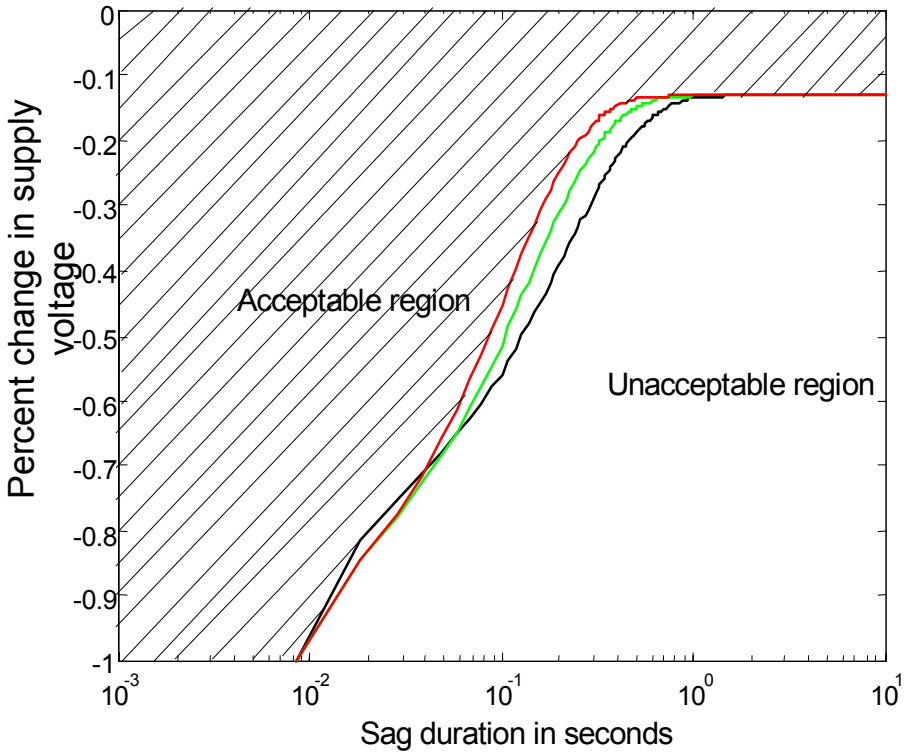

Figure 3.14 Power acceptability region for the case of multiple loads

Chapter 4

Voltage sag index

4.1 Introduction

Power quality indices often relate to the steady state phenomena, and relatively few relate to momentary events. However, many power quality engineers feel that bus voltage sags, a natural consequence of a highly interconnected transmission system, may be one of the most important type of power quality degradation, and a useful measure of the severity of these events is desirable. One of such metrics is the power acceptability curve, which is a graphic metric. The development of a numerical index that measures the compliance of an event with power acceptability curve is proposed.

A voltage sag index is a parameter that depicts the performance of a power system with reference to voltage sag. Power acceptability curves such as CBEMA curve (and the new version ITIC curve) is a magnitude-duration curve, indicating that the severity of a voltage sag event is a function of both magnitude and duration. In this chapter a voltage sag index based on the CBEMA technology is proposed. The proposed voltage sag index, thus employs both the magnitude and time duration information of the sag event in assessing the acceptability or otherwise of the event.

A graphical comparison of the proposed voltage sag index and other measures of severity of voltage disturbances such as energy served and sag energy indices are undertaken.

4.2 Development of the proposed voltage sag index

In most areas of engineering, it is important to use indices to measure or quantify the quality of performance. Consider Figure 4.1 in this matter. Point P represents an event $\Delta V = \Delta V_p$ and $T = T_p$ (shown as 'unacceptable' in Figure 4.1). As an index of power acceptability, it is proposed to vary the threshold V_T until the power acceptability curve passes through P. This is shown as dashed lines in Figure 4.1. Recall Equation (3.13) in Chapter 3, the equation of a CBEMA-like power acceptability curve for a given DC standard V_T and the two filter time constants a, b

$$\Delta V = \frac{V_T + A\left(e^{-aT} - e^{-bT}\right) - 1}{1 - e^{-bT}}. \tag{4.1}$$

Then, one sets V_T to V_{Tp} and in Equation (4.1) the results is

$$\Delta V_p = \frac{V_{T_p} + A\left(e^{-aT_p} - e^{-bT_p}\right) - 1}{1 - e^{-bT_p}}. \tag{4.2}$$

Isolating V_{Tp} yields

$$V_{T_p} = 1 + \Delta V_p\left(1 - e^{-bT_p}\right) + A\left(e^{-aT_p} - e^{-bT_p}\right). \tag{4.3}$$

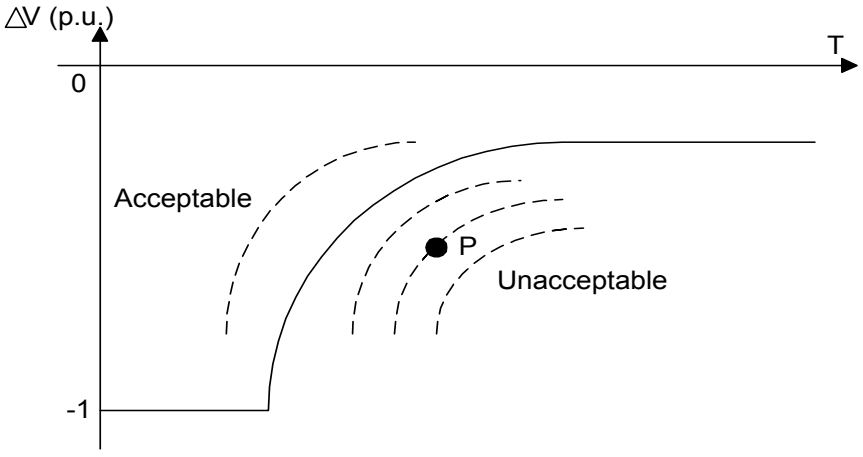

Figure 4.1 Graphic interpretation of an index of power acceptability for an event P

Consider the index V_{Tp}/V_T. If $V_{Tp}/V_T \geq 1$, the point P represents an acceptable event. It is a simple matter to show that the theoretical maximum of the index V_{Tp} / V_T is $1/V_T$. Hence, Figure 4.2 is a graphic depiction of a power acceptability index using the index I_{pa},

$$I_{pa} = V_{Tp} / V_T.$$

If one uses T_x as in Equation (3.14) in Chapter 3, it is a simple matter to show

$$I_{pa} = \frac{1}{V_T}\left(1+\Delta V_p\left(1-e^{-bT_p}\right)+\frac{e^{-bT_x}-V_T}{e^{-bT_x}-e^{-aT_x}}\left(e^{-aT_p}-e^{-bT_p}\right)\right) \tag{4.4}$$

This is an index of power acceptability for the event P.

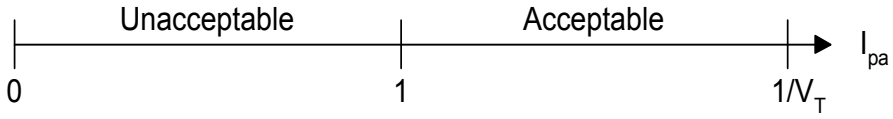

Figure 4.2 Proposed power acceptability index $I_{pa} = V_{T_p} / V_T$

4.3 Correlation of the proposed index to energy served

In the previous section, an index I_{pa} was proposed based on V_{TP}, a $V(t\rightarrow\infty)$ value extrapolated from the generalized CBEMA curve,

$$I_{pa} = V_{TP} / V_T.$$

As discussed above, if $1 \leq I_{pa} \leq 1/V_T$, where V_T is the voltage standard (i.e., V_T=0.87 per unit for the CBEMA curve) one concludes that P is an undervoltage event that lies in the acceptable range on the generalized CBEMA curve. For the standard CBEMA curve

$$1 \leq I_{pa} \leq 1.15 \text{ per unit.}$$

There are other measures of the severity of a sag event. One such measure is "energy served" (ES). Energy served refers to the integral of instantaneous power, *v(t)i(t)*, over an event. In signal processing, the usual assumption of a 1 Ω load is made, from which one obtains $v^2(t)$ as the instantaneous power. Therefore *ES* is

$$ES = \int_0^T v^2(t)dt.$$

In the case of actual field measurement, it is not very convenient to calculate this integral in detail. For this remark, an approximate *ES* is simply

$$ES = V^2T$$

Where *V* is the RMS value of *v(t)* in $0 < t < T$ and *T* is the duration of the event. To form an index,

$$ES = V^2_{actual,RMS}T \big/ V^2_{rated,RMS}T$$

or on a per unit basis

$$ES_{pu} = V^2_{actual,RMS}.$$

It is natural to ask the relationship between *ES* and the voltage sag index, I_{pa}. Evidently, as I_{pa} drops from $1/V_T$ to 1 and further to values smaller than 1; ES_{pu} drops from 100 percent to lower and lower values. The relationship between *ES* and I_{pa} is discussed further in this section.

The index of power acceptability proposed, I_{pa} is calculated for a set of voltage sag events obtained from the field. An empirical comparison of *ES* and I_{pa} can be obtained by examining actual field data. To this end, field data from a primary distribution system were obtained. The field data, assumed to be exemplary, are shown in Appendix D. The I_{pa} for the three phase data is obtained by applying the three phase voltage set to a six-pulse diode bridge rectifier system. The DC voltage obtained at the

load end, together with time duration of the sag obtained from the field data are passed to Equation (4.4) for the calculation of the I_{pa}. The *LC* filter design used is the same as the one used in the derivation of Equation (3.3) in Chapter 3. The CBEMA voltage standard of 0.87 p.u: is employed. Figure 4.3 depicts a plot of the voltage sag index, I_{pa} versus energy served, *ES,* for the field data evaluated. The energy served in this case is the sum of the energies delivered in all the three phases. Similar analysis and calculation is done for the phase 'a' of the field data. Figure 4.4 depicts the plot of the I_{pa} versus the energy served for phase 'a'.

Inspection of Figures 4.3 and 4.4 reveal the following observations:

- There is generally a monotonic relation between *ES* and I_{pa}. That is, when *ES* rises, I_{pa} rises and vice versa.
- The field measurements lie broadly on a rising curve as shown in Figures 4.3 and 4.4. However, *ES* is not truly the energy served because the integral of $v^2(t)$ was not evaluated. That is *ES* depicted in Figure 4.3 and 4.4 is approximate.
- For the three phase case, a mixed per unit index is plotted in which rated value is 300%.
- For the single phase case, only undervoltages are shown.
- For the three phase case, a few overvoltages occur, but it is possible that overvoltage in one phase is accompanied by undervoltage in another phase, and *ES* is less than 300%.

From Figure 4.3, the voltage sag event is said to be acceptable (at least in the sense of CBEMA) if the proposed index, $I_{pa}>1$ or when the $ES > 0.6$ p.u for the three phase system. For the single phase equivalent as shown in Figure 4.4, the acceptable region is $I_{pa}>1$ or $ES > 0.57$ *p.u*.

Now the salient question is, is there any advantage of working with I_{pa}? The following are the advantages and the disadvantages of I_{pa} and *ES*:

- *ES* is easier to calculate and instrument.
- I_{pa} is more theoretically 'correct' once CBEMA is accepted.
- I_{pa} is fully extendable to other criteria (e.g. speed, force criterion), but *ES* is not.
- The physical meaning of *ES* is based on energy. I_{pa} is voltage based
- Three phase implications favor I_{pa}.
- Sag duration is not captured in *ES*.

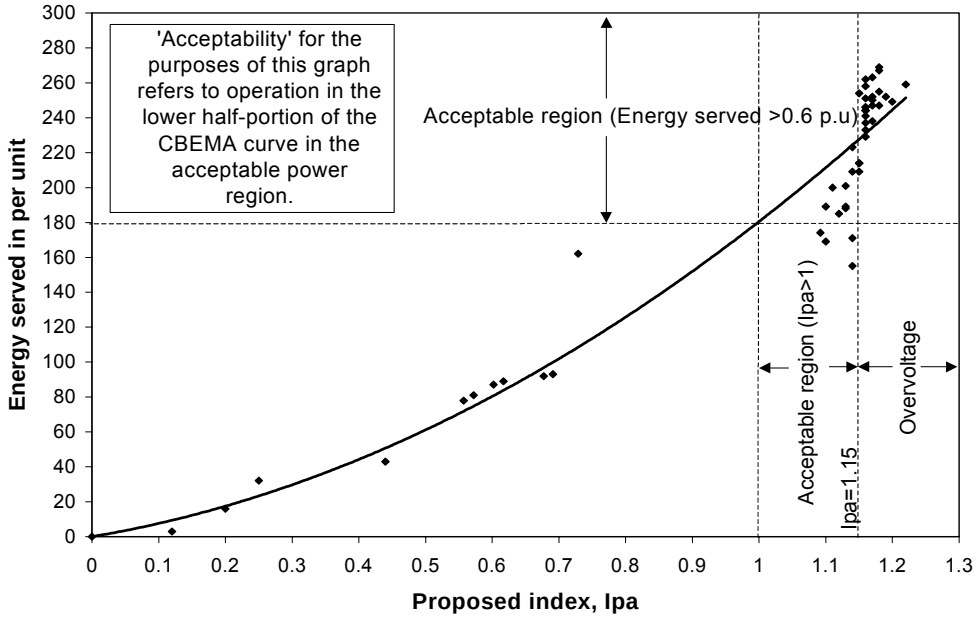

Figure 4.3 Proposed index, I_{pa} versus *ES* for the three phase system

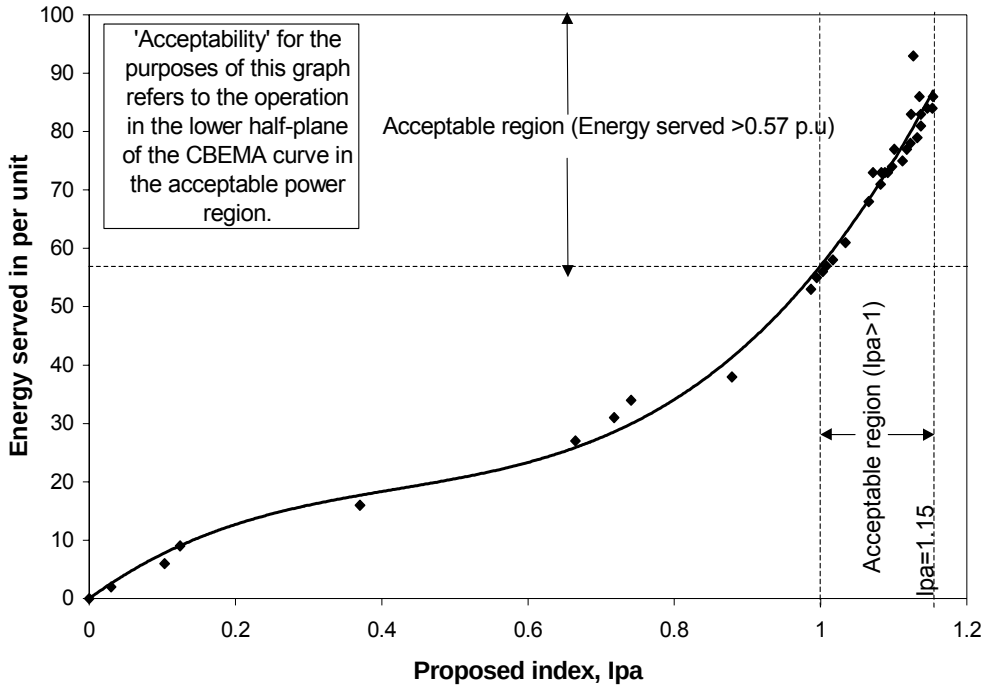

Figure 4.4 Proposed index, I_{pa} versus *ES* for the phase 'a' of the three phase system

4.4 Voltage sag index, I_{pa} versus sag energy index

In this section, the proposed voltage sag index, I_{pa} is compared graphically with another index of power acceptability, sag energy index (SEI), that is presently being used by a utility company. The intent is to establish if possible the relationship between I_{pa} and *SEI.*

Sag energy index literally represents the sum of voltage sag energies for all events measured at a given site during a given period. Mathematically, sag energy index is defined as

$$SEI = [(100 - ES_a) + (100 - ES_b) + (100 - ES_c)] \times [event\ duration]$$

where ES_a, ES_b, ES_c are the phase energy values. The phase energy values are computed as follows:

$$ES_a = \frac{\int_{event\_start}^{event\_end} V_{a\_actual}^2 dt}{\int_{event\_start}^{event\_end} V_{a\_rated}^2 dt} \times 100$$

$$ES_b = \frac{\int_{event\_start}^{event\_end} V_{b\_actual}^2 dt}{\int_{event\_start}^{event\_end} V_{b\_rated}^2 dt} \times 100$$

$$ES_c = \frac{\int_{event\_start}^{event\_end} V_{c\_actual}^2 dt}{\int_{event\_start}^{event\_end} V_{c\_rated}^2 dt} \times 100 .$$

These phase energy values are usually measured using electronic monitors in the field. This is done by subjecting the voltage sag event to 10-minute temporal aggregation. The most severe event within the 10-minute duration is recorded.

Sag energy index, *SEI* values are calculated from the field data shown in Appendix D and it is plotted against the proposed voltage sag index, $I_{pa.}$ In computing the *SEI* values events longer than 60 seconds, overvoltage events and transient events are not include. Also, voltage sag events longer than 15 cycles are calculated as a 15-cycle event. Further, phase energy values greater then 100% are limited to a maximum of 100%.

Figure 4.5 depicts a plot of voltage sag index, I_{pa} versus the values of *SEI* evaluated from the field data shown in Appendix D. From Figure 4.5, it is evident that I_{pa} and *SEI* have roughly a polynomial relationship. An acceptable region in the sense of CBEMA for I_{pa} is $I_{pa} > 1$. This region corresponds to *SEI* <14.

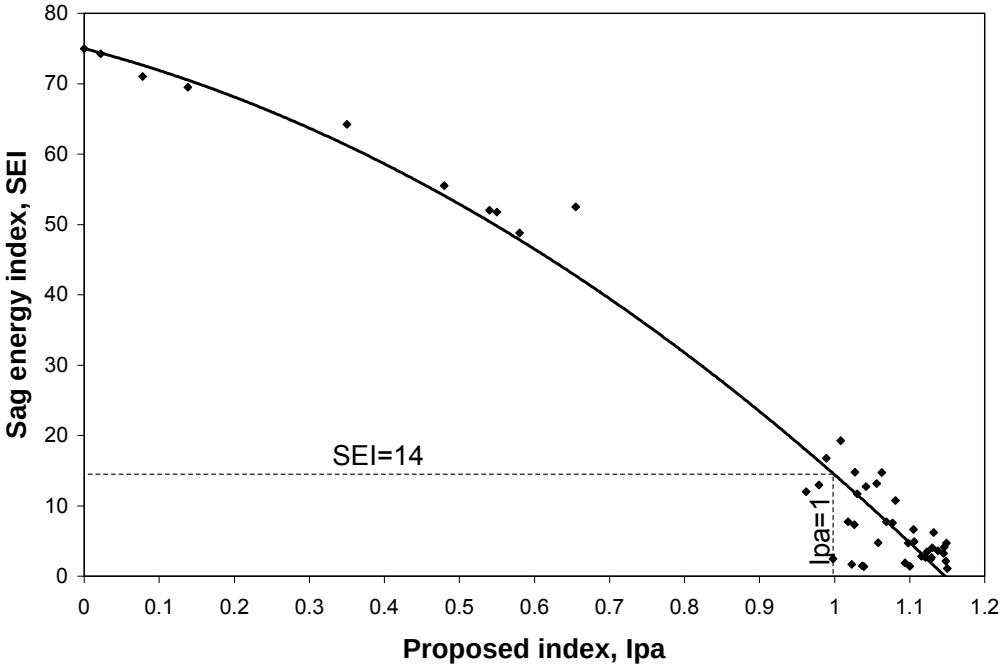

Figure 4.5 Proposed voltage sag index, I_{pa} versus *SEI* for the three phase system

Chapter 5

Conclusions and recommendations

5.1 Conclusions

The main conclusion of this work is that power acceptability curve for any industrial load can be constructed based on the concept of "power quality standard" and a knowledge of the model of the load. The "power quality standard" entails an ultimate criterion upon which an acceptability of distribution power supply can be made. If the industrial load is a rectifier type the applicable standard is the voltage standard: the minimum acceptable DC voltage at the output of the rectifier that will result in proper operation of the load. If the industrial load is a rotating type the standard is the machine speed. For an electromagnetic relay type, a force standard is used.

It is shown in this work that the CBEMA curve is based on the single phase rectifier load with DC threshold voltage of 0.87 per unit in the undervoltage region. The "formula" for the undervoltage region of the CBEMA curve is developed and found to be

$$V_{end} = \frac{0.87 - 0.288\ e^{-1.06\ T} - 0.712\ e^{-23.7\ T}}{1 - e^{-23.7\ T}}\ .$$

Other CBEMA-like power acceptability curves are developed for unbalanced three phase issues and rotating loads. Double exponential equations describing the curves are developed. The issue of power acceptability for the case of multiple loads with different power acceptability curves is addressed. It is proposed that the overall acceptable region for the case of multiple loads must be the intersection of the individual acceptable regions. For the case of a rotating load driving different loads with different power acceptability curves, it is proposed that the power acceptability curve with

narrowest acceptable operating region must be applied. The point-on-the wave where a voltage sag event occurs play a great role in defining the acceptable region for the case of AC contactor loads.

The analysis of power acceptability curves from the point of view of energy disturbance concept, an objective of this work is captured. It became clear from the analysis that the shape of the power acceptability curves cannot be modeled based on the disturbance energy concept.

An index based on compliance of power acceptability curve is proposed. The proposed index is a function of voltage sag magnitude and duration since power acceptability curves are function of both sag magnitude and duration. The proposed voltage index, I_{pa} is defined as

$$\boldsymbol{I_{pa}} = \frac{1}{V_T}\left(1+\Delta V_p\left(1-e^{-bT_p}\right)+\frac{e^{-bT_x}-V_T}{e^{-bT_x}-e^{-aT_x}}\left(e^{-aT_p}-e^{-bT_p}\right)\right)$$

Unbalanced and balanced three phase issues are accounted for in the proposed power acceptability index. The comparisons of the index with other measures of the severity of voltage sag events are illustrated.

5.2 Recommendations

It is recommended that the proposed method to design power acceptability curves is extended to other industrial load types that this work failed to address. These include forced commutated rectifiers, temperature sensors and other protective relays.

After a suitable period of evaluating the proposed method, it may be possible to use this technique as a recommended practice in industry.

References

[1] R. S. Thallam, G.T. Heydt, “Power acceptability and voltage sag indices in the three phase sense,” Paper presented at Panel Session on “Power Quality-Voltage Sag Indices,” IEEE PES Summer Meeting, July 2000, Seattle, WA.

[2] R. Waggoner, “Understanding the CBEMA curve,” Electrical Construction and Maintenance, Vol. 90, No. 10, October 1991, pp. 55-57.

[3] G. Heydt, W. Jewell, “Pitfalls of electric power quality indices,” IEEE Transactions on Power Delivery, Vol. 13, No. 2, April 1998, pp. 570-578.

[4] G. T. Heydt, Electric Power Quality, Stars in a Circle Publication, Scottsdale, AZ 1995.

[5] D. L. Brooks, R. C. Dugan, M. Waclawiak, A Sundaram, “Indices for assessing utility distribution systems RMS variation performance,” IEEE Transactions on Power Delivery, Vol. 131, January 1998, pp. 254-259.

[6] G. T. Heydt, G. G. Karady, B. Cummings, J. Tang, “Improved application of power acceptability curves and their application to three-phase loads,” Journal of Electric Machines and Power Systems, July 1999, Vol. 27, pp. 737-751.

[7] M. Stephens, J. McComb, “Power quality in chiller systems,” Power Quality Assurance, September/October 2000, pp. 42-52.

[8] D. D. Sabin, T. E. Grebe, A. Sundaram, “RMS voltage variation statistical analysis for a survey of distribution system power quality performance,” IEEE Power Engineering Society 1999 Winter Meeting, Vol. 2, January 1999, pp. 1235-1240.

[9] A. Dettloff, “Power quality performance component of the special manufacturing contracts between energy provider and customer,” IEEE Power Engineering Society 2000 Summer Meeting, Vol. 2, July 2000, pp. 912.

[10] G. T. Heydt, “Electrical power quality: a tutorial introduction,” IEEE Computer Applications in Power, Vol. 111, January 1998, pp. 15-19.

[11] M. G. Ennis, R. P. O’Leary, “Solid state transfer switches: the quarter-cycle myth,” Power Quality Assurance, December 2000, pp. 10-16.

[12] N. S. Tunaboylu, E. R. Collins Jr., S. W. Middlekauff, R. L. Morgan, “Ride-through issues for DC motor drives during voltage sags,” IEEE Industrial Application Society Southeast Conference, July 1995, pp. 52-58.

[13] L. Ching-Yin, C. Bin-Kwie, L. Wei-Jen, H. Yen-Feng, “Effects of various unbalanced voltages on the operation performance of an induction motor under the same

voltage unbalance factor condition," IEEE Industrial and Commercial Power Systems Technical Conference, July 1997, pp. 51-59.

[14] E. Collins, R. Morgan, "A three phase sag generator for testing industrial equipment," IEEE Transactions on Power Delivery, Vol. 11, No. 1, January 1996, pp. 526 - 532.

[15] D. Koval, "Computer performance degradation due to their susceptibility to power supply disturbances," Conference Record, IEEE Industry Applications Society Annual Meeting, October 1989, Vol. 2, pp. 1754 - 1760.

[16] M. Bollen, L. Zhang, "Analysis of voltage tolerance of AC adjustable-speed drives for three-phase balanced and unbalanced sags," IEEE Transactions on Industry Applications, Vol. 36, No. 3, May-June 2000, pp. 904 -910.

[17] E. Collins, A. Mansoor, "Effects of voltage sags on AC motor drives," Proceedings of the IEEE Technical Conference on the Textile, Fiber and Film Industry, May 1997, pp. 9 - 16.

[18] J. C. Gomez, M. M. Morcos, C. Reineri, G. Campetelli, "Induction motor behavior under short interruptions and voltage sags," IEEE Power Engineering Review, Vol. 21, No. 2, February 2001, pp. 11-15.

[19] J. Kyei, R. Ayyanar, G. Heydt, R. Thallam, J. Blevins, “The design of power acceptability curves,” Submitted for publication, IEEE Power Engineering Society, May 2001.

[20] E. R. Collins, Jr., M. A. Bridgwood, “ The impact of power system disturbances on AC-coil contactors,” IEEE Technical Conference on Textile, Fiber and Film Industry, June 1997, pp. 2-6.

[21] A. Kelley, J. Cavaroc, J. Ledford, L. Vassalli, “Voltage regulator for contactor ride through,” IEEE Transactions on Industry Applications, Vol. 36, No. 2, March 2000, pp. 697-703.

[22] M. F. McGranaghan, D. R. Mueller, M. J. Samotyj, “Voltage sags in industrial systems,” IEEE Transactions on Industrial Applications, Vol. 29, No. 2, March 1993, pp. 397-403.

[23] E. R. Collins, Jr., F. Zapardiel, “An experimental assessment of AC contactor behavior during voltage sags,” Proceedings of IEEE International Symposium on Industrial Electronics, Vol. 2, July 1997, pp. 439-444.

[24] J. Kyei, G. Heydt, R. Ayyanar, R. Thallam, J. Blevins, “The design of power acceptability curves,” Submitted for publication, Northern American Power Symposium, May 2001.

Appendix A

Newton’s method for solving nonlinear system of equations

A.1 Analysis

For a three phase six-pulse diode bridge rectifier load operating under a faulting AC voltage supply, the equation of the DC voltage response is given by the approximation

$$V_{dc}(t) = V_{end} + Ae^{-bt} + Be^{-ct}. \quad \text{(A.1)}$$

At time $t=0$,

$$B = 1 - V_{end} - A. \quad \text{(A.2)}$$

Substituting Equation (A.2) into Equation (A.1) results in

$$V_{dc}(t) = V_{end} + Ae^{-bt} + (1-V_{end} - A)e^{-ct}. \quad \text{(A.3)}$$

For a voltage standard of $V_{dc} = 0.87$ and the set of solutions (t, V_{end}) given by (0.00833, 0), (0.1, 0.6) and (1, 0.77), the system of equations below can be obtained from Equation (A.3),

$$0.87 = Ae^{-0.00833b} + (1 - A)e^{-0.00833c} \quad \text{(A.4)}$$

$$0.87 = 0.6 + Ae^{-0.1b} + (1 - A - 0.6)e^{-0.1c} \quad \text{(A.5)}$$

$$0.87 = 0.77 + Ae^{-b} + (1 - A - 0.77)e^{-c}. \quad \text{(A.6)}$$

The constants A, b and c in Equations (A.4), (A.5) and (A.6) are obtained by solving the system of nonlinear equations using Newton's method.

A.2 Matlab code for solving the system of equations using Newton's method

```
%This program solves a system of three nonlinear equations
%Using Newton's method.

%Program begins
A=(.27-0.4*exp(-.1*c))/(exp(-0.1*b)-exp(-0.1*c));
f1=.1-A*exp(-b*1)-(.23-A)*exp(-c*1);
f1=f1*f1;
f2=0.87-a*exp(-b*0.00833)-(1-a)*exp(-c*0.00833);
f2=f2*f2;
e=0.0001;
b=b+e;
```

```
A=(.27-0.4*exp(-0.1*c))/(exp(-0.1*b)-exp(-0.1*c));
f1b=.1-A*exp(-b*1)-(.23-A)*exp(-c*1);
f1b=f1b*f1b;
f2b=0.87-A*exp(-b*0.00833)-(1-A)*exp(-c*0.00833);
f2b=f2b*f2b;
b=b-e;
c=c+e;
A=(.27-0.4*exp(-0.1*c))/(exp(-0.1*b)-exp(-0.1*c));
f1c=.1-A*exp(-b*1)-(.23-A)*exp(-c*1);
f1c=f1c*f1c;
f2c=0.87-A*exp(-b*0.00833)-(1-A)*exp(-c*0.00833);
f2c=f2c*f2c;
j=[(f1b-f1)/e, (f1c-f1)/e;(f2b-f2)/e, (f2c-f2)/e];
j=inv(j);
c=c-e;
bc=[b; c]-j*[f1; f2]
f1
f2
b=[1,0]*bc;
c=[0,1]*bc;
%Program ends
```

Appendix B

Power acceptability curve for three phase rectifier: phase-to-phase-ground fault

A three phase six-pulse diode bridge rectifier subjected to a phase-to-phase-ground fault is simulated and the power acceptability curve for this condition is constructed. The procedure is the similar to that of the phase-to-ground fault. The equation of the power acceptability curve is obtained as

$$V_{end} = \frac{0.87 - 0.25e^{-0.85t} - 0.75e^{-7.25t}}{1 - e^{-7.25t}}.$$

The power acceptability curve for the equation shown above is depicted in Figure B.1.

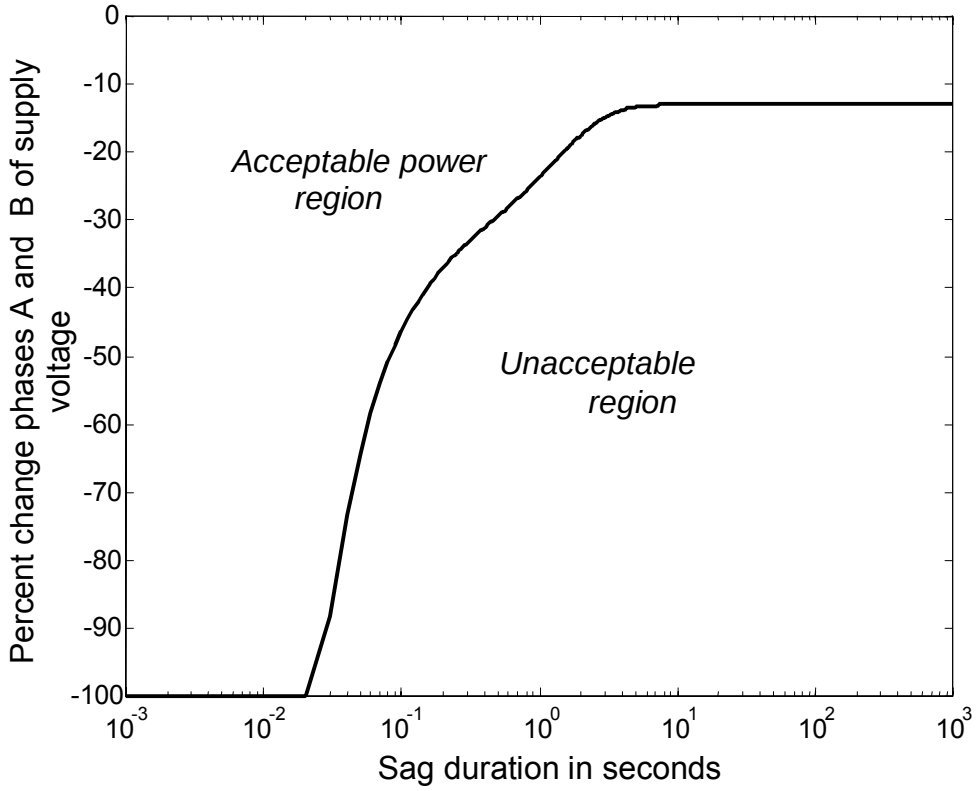

Figure B.1 Power acceptability curve for a three phase rectifier load with a phase-to-phase-to-ground fault at phases 'a' and 'b', 87% V_{dc} voltage standard

Appendix C

Matlab code for the simulation of induction motor load

```
%This program simulates an induction motor load under a three phase fault.
% The rating of the motor load is 30hp, 480V, 4 pole, 60Hz and 2% slip.
%The load driven in this case is a constant load torque.

%Program begins

% Program input
r1=0.22;  % rotor resistance in ohms
r2=0.22;  % stator resistance in ohms
x1=0.34;  % rotor reactance in ohms(60Hz)
x2=0.37;  % stator reactance in ohms(60Hz)
xm=50;  %core and magnetizing branch reactance in ohms (60Hz)
rm=500;  % core and magnetizing branch resistance in ohms
J=.38;  % moment of inertia of the induction motor load
Ws=60*pi;  % synchronous speed of the induction machine in radians per second
W(1)=0.98*Ws;   % rated motor shaft speed in radians per second
t(1)=0.0;   % initial time
t0=0.0001;  % simulation step size

for i=1:1:500; %iteration begins
  s=(Ws-W(i))/Ws; % motor slip at any time
   % calculation of stator current
  a1=(rm*xm^2)/(rm^2+xm^2);
  a2=(xm*rm^2)/(rm^2+xm^2);
  b1=r2/s;
  b2=x2;
  c1=a1*b1-a2*b2;
  c2=a1*b2+a2*b1;
  d1=a1+b1;
  d2=a2+b2;
  f1=c1*d1+c2*d2;
  f2=c2*d1-c1*d2;
  e1=d1^2+d2^2;
  g1=f1/e1;
  g2=f2/e1;
  h1=g1+r1;
  h2=g2+x1;
  k1=sqrt(h1^2+h2^2);

  if i==1
    V=277.1;   % rated phase voltage
  else
    V=0.5*277.1; % voltage sag
  end
                        I1=V/k1;  % current flowing in the stator winding
  I2=(sqrt(a1^2+a2^2)/sqrt(d1^2+d2^2))*I1;  %rotor current
  Te=3*(I2^2)*b1/Ws;  % shaft torque
```

```
  if i==1
    T=Te;  % calculation of load torque
  end

  err=T-Te;  % torelance
  if ((i>=5)&(err<=0.00001))
    Te=T;
  end

  K=(Te-T)/J;  %Load torque constant

  t(i+1)=i*t0;  %running time
  W(i+1)=W(i)+K*t(i+1);  %shaft speed updated
End % Iteration ends

%Program output
plot(t,W)
xlabel('disturbance duration in seconds')
ylabel('speed')
title('Induction motor speed curve for voltage sags')
grid

%Program ends
```

Appendix D

Field measurements from primary power distribution system

Data obtained from field measurements of a distribution system are depicted in Tables D.1. Items shown in Tables D.1 are the average voltage measurements all the three phases and their associated energy served in percentages. Also indicated is the sag duration, T in seconds. The energy served ES is defined as

$$ES = V^2_{actual,RMS}T \big/ V^2_{rated,RMS}T \ .$$

Table D.1 Data obtained from field measurements

Sag duration (seconds)	Percent average voltage			Percent energy served		
	V_a	V_b	V_c	ES_a	ES_b	ES_c
0.050	86	98	87	73	96	75
0.084	87	86	97	75	74	95
0.067	93	91	99	86	82	99
0.083	76	96	76	58	93	58
0.083	92	89	93	84	80	87
0.083	98	85	83	96	72	69
0.049	88	99	88	77	98	76
0.068	86	85	98	74	71	96
0.049	93	91	100	86	82	100
0.083	75	96	75	57	93	57
0.066	91	89	95	83	79	89
0.067	97	82	81	94	68	65
0.049	86	98	88	73	96	77
0.083	92	89	93	84	80	86
0.034	86	98	87	75	96	75
0.068	97	88	87	94	77	76
0.067	86	85	98	74	72	96
0.067	93	91	100	86	83	100

Table D.1 Data obtained from field measurements (continued)

Sag duration (seconds)	Percent average voltage			Percent energy served		
	V_a	V_b	V_c	ES_a	ES_b	ES_c
0.066	97	84	81	94	70	65
0.016	90	100	91	80	99	83
3.204	2	1	1	2	1	0
0.133	47	84	88	26	70	78
0.099	40	85	89	17	73	79
0.098	89	98	89	80	96	79
0.668	89	88	96	79	77	93
0.166	88	88	96	77	77	93
0.149	82	77	86	68	60	73
0.067	100	101	79	99	102	63
0.017	91	101	92	82	102	84
0.034	101	79	102	102	63	104
0.034	78	99	100	60	98	100
0.016	98	100	75	97	100	57
0.133	47	90	94	27	76	86
0.117	47	90	94	29	82	89
0.083	90	100	90	81	100	82
0.551	89	89	99	80	79	98
0.166	89	89	99	80	80	99
0.133	82	76	86	68	58	75
0.049	91	91	99	83	82	98
0.615	22	23	18	16	17	10
2.036	7	7	6	6	6	4
0.016	103	68	101	106	46	102
2.853	11	13	13	9	11	2

Table D.1 Data obtained from field measurements (continued)

Sag duration (seconds)	Percent average voltage			Percent energy served		
	V_a	V_b	V_c	ES_a	ES_b	ES_c
0.150	84	96	95	71	92	89
0.067	72	59	97	53	37	95
0.066	73	59	98	55	38	96
0.585	51	40	61	27	17	46
0.066	74	57	98	56	36	96
0.100	89	87	91	79	76	83
0.034	86	98	86	73	97	74
0.099	61	99	98	38	98	97
0.568	56	98	98	31	95	97
0.099	88	86	91	77	75	82
0.034	96	102	93	93	103	86
3.405	0	0	0	0	0	0
68.64	58	59	58	35	35	35
62.09	54	55	54	30	31	31
57.94	54	55	55	31	31	31
18.39	48	48	48	26	26	26
0.016	80	81	81	64	66	65
0.016	85	85	85	71	71	72
0.017	84	84	84	70	71	72
23.24	53	54	54	29	30	30
0.017	72	71	72	52	51	52
1.822	91	92	92	83	85	84
1.97	91	92	92	83	85	84
1.904	91	92	92	83	85	84